

P-73

NASA
Contractor Report 179620

AVSCOM
Technical Report 87-C-16

LEWIS
GRANT
10-31
79447

A Simplified Computer Solution for the Flexibility Matrix of Contacting Teeth for Spiral Bevel Gears

(NASA-CR-179620) A SIMPLIFIED COMPUTER
SOLUTION FOR THE FLEXIBILITY MATRIX OF
CONTACTING TEETH FOR SPIRAL BEVEL GEARS
Final Report (Northwestern Univ.) 73 p
Avail: NTIS BC A04/MF A01

N87-23977

Unclass
0079447

CSCD 131 G3/37

C.Y. Hsu and H.S. Cheng
Northwestern University
Evanston, Illinois

June 1987

Prepared for
Lewis Research Center
Under Grant NAG-3143

NASA
National Aeronautics and
Space Administration



TABLE OF CONTENTS

	Page
CHAPTER	
I INTRODUCTION.....	1
II ELASTIC COEFFICIENTS.....	2
2.1 Deflection of Tooth Fixed on Root Cone.....	2
2.2 Deflection of Wheel and Shaft.....	3
2.2.1 Deflections Due to Bending Moment.....	4
2.2.2 Deflections Due to Shearing Strain.....	11
2.2.3 Deflections Due to Axial Force.....	16
2.2.4 Deflections Due to Torsion.....	18
III DISCUSSION OF RESULTS.....	32
3.1 Comparison with Charles Chao's Results.....	32
3.2 Effect of Mass and Moment of Inertia.....	33
3.3 Effect of Stiffness.....	33
3.4 Effect of Damping Coefficient.....	34
IV CONCLUSIONS.....	41
REFERENCES.....	43
NOMENCLATURE.....	45
APPENDIX A - TWO SAMPLES OF INPUT DATA FOR SAPIV	48
APPENDIX B - DEFLECTION AND SLOPE AT POINT B	66

CHAPTER I

INTRODUCTION

In order to calculate the dynamic loads between contacting teeth of spiral bevel gears, it is necessary to compute first the elastic deformation of the tooth contacting surface under an unit normal load located at any arbitrary point on the surface. This was accomplished by Chao(1) using the finite element method. To insure accuracy, the finite element method was employed not only for the gear tooth but also for the gear wheel, hub and shaft. Such an approach necessitates the use of a large number of elements, and the computer cost was found to be prohibitive.

A simplified method is developed in this report to obtain the flexibility matrix, i.e., the deflection along the direction normal to the surface at each grid point on the tooth face due to an unit normal force acting on this point. In this analysis, an existing finite element code SAPIV was used to compute the deformation of the tooth itself. For the deformation of the gear wheel and shaft, conventional beam theory is employed. The total deformation is obtained by using the principle of superposition.

CHAPTER II

ELASTIC COEFFICIENTS

In order to obtain the deflection in the normal direction due to an unit normal force acting on a given grid point(Fig. 2-1), one can separate the gear into two parts: (1) tooth (2) wheel and shaft(Fig. 2-2). After obtaining the deflections from the above two parts, one can superimpose them to obtain the total deflection. Then the deflection in the normal direction at each grid point on the tooth face can be determined.

2.1 Deflection of Tooth Fixed on Root Cone

By fixing the root of the tooth, the finite element program SAPIV can be used to calculate the displacements of each grid point on the tooth surface for an unit normal load applied at any arbitrary grid point. In this calculation, three dimensional solid elements(eight node brick) are used. Fig. 2-3 shows the node number of a typical spiral bevel tooth which has a profile geometry indentical to that used by Chao(1). Appendix A gives two samples of input data for SAPIV.

2.2 Deflection of Wheel and Shaft

Let us consider the wheel and shaft as a beam. There are two axial planes perpendicular to each other and a transverse plane for the pinion or gear shaft as shown in Fig. 2-4(p. 25) for calculating the displacements in the xy plane. The boundary conditions are (see Fig. 2-5):

$$(D_y)_C = (D_y)_D = 0$$

$$(D_x)_C = 0 \tag{2.1}$$

$$(\theta_x)_E = 0$$

where $(D_y)_C$ is the displacement of point C along the y axis and $(\theta_x)_E$ is the angular displacement about the x axis at point E.

The unit normal force acting at any grid point G (Fig. 2-6) can be replaced by a set of forces and couples applied at the center of the cross section cut by the transverse plane (Fig. 2-4) through the grid point. The principle of superposition is applied here, and the deflection due to the force or the couple can be computed separately as shown in the following sections. These deflections can then be added algebraically to obtain the total deflection.

2.2.1 Deflections Due To Bending Moment

Fig. 2-7 is the free body diagram the unit normal force acting at a grid point on the gear contacting surface has been replaced by a set of forces and couples applied on the center of the cross section cut by the transverse plane through the grid point at a distance L from the y axis.

To obtain the deflection and slope at L , the beam is divided into 3 portions.

$$(1) \quad b \leq x < d$$

Considering the force equilibrium of the portion of the beam between B and E (Fig. 2-8), one obtains

$$M_2 = P(b - L) - M_0 \quad (2.2)$$

The moment of inertia of the cross sectional area with respect to the neutral axis is

$$I_1 = \frac{\pi(r_s^4 - r_i^4)}{4} \quad (2.3)$$

To obtain the deflection and slope at B due to the force P and moment M_2 , one can consider the deflection owing to P or M_2 separately. Referring to beam deflection table (2) and using the principle of superposition the

following results are obtained

$$y_B = \frac{b-c}{6EI_1} [2P(c-b)(d-b) + M_2(2d-3b+c)] \quad (2.4)$$

$$\begin{aligned} y'_B = \frac{1}{6EI_1} [& P(c-b)(2d-3b+c) + \\ & 2M_2(d+2c-3b)] \end{aligned} \quad (2.5)$$

where E is the modulus of elasticity.

Appendix B shows a detailed derivation of the deflection and slope at point B by solving differential equation of the elastic line B C D E.

$$(2) \quad a < L < x < b$$

Fig 2-9 is the free body diagram for the forces acting on the portion of the beam to the right of point L. One obtains

$$M_3 = P(x-L) - M_0 \quad (2.6)$$

Radius of pitch cone on the cross section passed by the transverse plane at a distance x from the y axis is

$$r_p = x \tan \theta_p \quad (2.7)$$

where θ_p is the pitch angle.

The moment of inertia of the cross-sectional area with respect to the neutral axis at a distance x from the y axis is

$$I_3 = \frac{\pi(x^4 \tan^4 \theta_p - r_i^4)}{4} \quad (2.8)$$

The differential equation is

$$\begin{aligned} y'' &= -\frac{M_3}{EI_3} \\ &= \frac{-4P}{\pi E \tan^4 \theta_p} \left[\frac{x - (L + \frac{M_0}{P})}{x^4 - \frac{r_i^4}{\tan^4 \theta_p}} \right] \end{aligned} \quad (2.9)$$

Let

$$A_5 = \frac{-4P}{\pi E \tan^4 \theta_p} \quad (2.10)$$

$$A_6 = L + \frac{M_0}{P} \quad (2.11)$$

$$A_7 = \frac{r_i^4}{\tan^4 \theta_p} \quad (2.12)$$

If $r_i \neq 0$

$$y' = A_5 \int \left(\frac{x - A_6}{x^4 - A_7^4} \right) dx + C_5 \quad (2.13)$$

$$y' = A_5 \int \left(\frac{D_1}{x - A_7} + \frac{D_2}{x + A_7} + \frac{D_3 x + D_4}{x^2 + A_7^2} \right) dx + C_5 \quad (2.14)$$

$$= A_5 \left[D_1 \ln|x - A_7| + D_2 \ln|x + A_7| + \frac{D_3}{2} \ln(x^2 + A_7^2) + \right.$$

$$\left. \frac{D_4}{A_7} \tan^{-1} \frac{x}{A_7} \right] + C_5$$

where

$$D_1 = -\frac{1}{4A_7^3} (A_7 - A_6) \quad (2.15)$$

$$D_2 = \frac{1}{4A_7^3} (A_6 + A_7) \quad (2.16)$$

$$D_3 = -\frac{1}{2A_7^2} \quad (2.17)$$

$$D_4 = \frac{A_6}{2A_7^2} \quad (2.18)$$

C_5 can be determined from the condition

$$y' = y'_B \quad \text{at } x = b$$

One obtains

$$C_5 = y_B - A_5[D_1 \ln|b - A_7| + D_2 \ln|b + A_7| + \quad (2.19)$$

$$\frac{D_3}{2} \ln(b^2 + A_7^2) + \frac{D_4}{A_7} \tan^{-1} \frac{b}{A_7}]$$

Separating variables and integrating one obtains

$$y = A_5[D_1(x - A_7) \ln|x - A_7| - D_1(x - A_7) + \quad (2.20)$$

$$D_2(x + A_7) \ln|x + A_7| - D_2(x + A_7) +$$

$$\frac{D_3 x}{2} \ln(x^2 + A_7^2) - D_3 x + D_3 A_7 \tan^{-1} \frac{x}{A_7} +$$

$$\frac{D_4 x}{A_7} \tan^{-1} \frac{x}{A_7} - \frac{D_4}{2} \ln\left[\left(\frac{x}{A_7}\right)^2 + 1\right] + C_5 x + C_6$$

At $x = b$, $y = y_B$, one obtains

$$C_6 = y_B - A_5[D_1(b - A_7)[\ln|b - A_7| - 1] + \quad (2.21)$$

$$D_2(b + A_7)[\ln|b + A_7| - 1] + \frac{D_3 b}{2} [\ln(b^2 + A_7^2) -$$

$$2] + \tan^{-1} \frac{b}{A_7} (D_3 A_7 + \frac{D_4 b}{A_7}) - \frac{D_4}{2} \ln\left[\left(\frac{b}{A_7}\right)^2 + 1\right] -$$

$$C_5 b$$

Setting $x = L$, one obtains the deflection and slope of point L

$$y_L = A_5 \{ D_1 (L - A_7) [\ln |L - A_7| - 1] + \quad (2.22)$$

$$D_2 (L + A_7) [\ln |L + A_7| - 1] + \frac{D_3 L}{2} [\ln (L^2 + A_7^2) -$$

$$2] + \tan^{-1} \frac{L}{A_7} (D_3 A_7 + \frac{D_4 L}{A_7}) - \frac{D_4}{2} \ln [(\frac{L}{A_7})^2 + 1] \} +$$

$$C_5 L + C_6$$

$$y'_L = A_5 [D_1 \ln |L - A_7| + D_2 \ln |L + A_7| + \quad (2.23)$$

$$\frac{D_3}{2} \ln (L^2 + A_7^2) + \frac{D_4}{A_7} \tan^{-1} \frac{L}{A_7}] + C_5$$

$$\text{If } r_i = 0$$

$$y' = A_5 \int \left(\frac{x - A_6}{x^4} \right) dx + C'_5$$

$$= - \frac{A_5}{6x^3} (3x - 2A_6) + C'_5 \quad (2.24)$$

$$y = \frac{A_5}{6x^2} (3x - A_6) + C'_5 x + C'_6 \quad (2.25)$$

By knowing $y' = y'_B$ and $y = y_B$ at $x = b$, one obtains

$$c'_5 = y'_B + \frac{A_5}{6b^3}(3b - 2A_6) \quad (2.26)$$

$$c'_6 = y_B - \frac{A_5}{6b^2}(3b - A_6) - c'_5 b \quad (2.27)$$

Replacing x by L into equations (2.24) and (2.25)

$$y_L = \frac{A_5}{6L^2}(3L - A_6) + c'_5 L + c'_6 \quad (2.28)$$

$$y'_L = -\frac{A_5}{6L^3}(3L - 2A_6) + c'_5 \quad (2.29)$$

$$(3) \quad a < x < L$$

Setting $x = a$ into equations (2.14) and (2.20) (or (2.24) and (2.25) as $r_i = 0$), one obtains y_A and y'_A .

Then

$$y_L = y_A + (L - a)y'_A \quad (2.30)$$

$$y'_L = y'_A \quad (2.31)$$

The displacement of grid point G can be calculated from the displacement of L by virtue of the fact that

G and L lie in the same transverse plane which is assumed to remain plane after deformation.

Fig. 2-10 shows how the grid point G moves to the final position following the displacement of point L.

Here

$$D = |y_L| \quad (2.32)$$

$$\theta = |y'_L| \quad (2.33)$$

Hence, one can obtain the displacement of the grid point G by rotation about point L and translation.

2.2.2 Deflections Due to Shearing Strain

Referring to Fig. 2-7 again, one can divide the beam into 3 portions for derivation.

$$(1) \quad b < x < c$$

$$I_1 = \frac{\pi(r_s^4 - r_i^4)}{4}$$

The maximum shear stress τ_{\max} is induced on neutral plane. So

$$b_1 = 2(r_s - r_i) \quad (2.34)$$

$$\tau_{\max} = \frac{P}{I_1 b_1} \int_{r_i}^{r_s} y dA$$

$$= \frac{8(r_s^3 - r_i^3)P}{3\pi b_1(r_s^4 - r_i^4)} \quad (2.35)$$

Then the slope of the elastic line becomes

$$\frac{dy}{dx} = \frac{\tau_{\max}}{G} \quad (2.36)$$

where G is the shear modulus.

Integrating

$$y = \frac{\tau_{\max}}{G}x + C_7 \quad (2.37)$$

Using the condition: $y = 0$ at $x = c$, one obtains

$$C_7 = - \frac{\tau_{\max}c}{G} \quad (2.38)$$

Then the deflection of point B becomes

$$y_B = \frac{\tau_{\max}b}{G} + C_7 \quad (2.39)$$

$$(2) \quad a < L < x < b$$

Referring to Fig. 2-9

$$r_p = x \tan \theta_p$$

$$I_2 = \frac{\pi(x^4 \tan^4 \theta_p - r_i^4)}{4} \quad (2.40)$$

$$b_2 = 2(r_p - r_i) \quad (2.41)$$

$$\begin{aligned} \tau_{\max} &= \frac{P}{I_2 b_2} \int_{r_i}^{r_p} y dA \\ &= \frac{P(r_p^2 + r_p r_i + r_i^2)}{3I_2} \end{aligned} \quad (2.42)$$

$$\begin{aligned} \frac{dy}{dx} &= \frac{\tau_{\max}}{G} \\ &= \frac{4P(r_p^2 + r_p r_i + r_i^2)}{3\pi G(r_p^4 - r_i^4)} \end{aligned} \quad (2.43)$$

$$dx = \frac{dr_p}{\tan \theta_p} \quad (2.44)$$

Let

$$A_8 = \frac{4P}{3\pi G \tan \theta_p} \quad (2.45)$$

$$r_{pB} = b \tan \theta_p \quad (2.46)$$

$$r_{pL} = L \tan \theta_p \quad (2.47)$$

If $r_i \neq 0$

$$y = A_8 \int \left(\frac{r_p^2 + r_i r_p + r_i^2}{r_p^4 - r_i^4} \right) dr_p + C_8$$

$$= A_8 [D_5 \ln|r_p - r_i| + D_6 \ln|r_p + r_i| + \frac{D_7}{2} \ln(r_p^2 + r_i^2)] + C_8 \quad (2.48)$$

where

$$D_5 = \frac{3}{4r_i} \quad (2.49)$$

$$D_6 = -\frac{1}{4r_i} \quad (2.50)$$

$$D_7 = -\frac{1}{2r_i} \quad (2.51)$$

Using the condition: $y = y_B$ at $x = b$, one obtains

$$C_8 = y_B - A_8 [D_5 \ln|r_{pB} - r_i| + D_6 \ln|r_{pB} + r_i| + \frac{D_7}{2} \ln(r_{pB}^2 + r_i^2)] \quad (2.52)$$

Setting $x = L$, one obtains the deflection and slope at point L

$$y_L = A_8 [D_5 \ln|r_{pL} - r_i| + D_6 \ln|r_{pL} + r_i| + \frac{D_7}{2} \ln(r_{pL}^2 + r_i^2)] + C_8 \quad (2.53)$$

$$y'_L = \frac{4P(r_{pL}^2 + r_{pL}r_i + r_i^2)}{3\pi G(r_{pL}^4 - r_i^4)} \quad (2.54)$$

If $r_i = 0$

$$\begin{aligned} y &= A_8 \int \frac{1}{r_p^2} dr_p + C_8' \\ &= -\frac{A_8}{r_p} + C_8' \end{aligned} \quad (2.55)$$

Using the condition: $y = y_B$ at $x = b$, one obtains

$$C_8' = y_B + \frac{A_8}{r_{pB}} \quad (2.56)$$

Setting $x = L$, the deflection and slope at point L become

$$y_L = -\frac{A_8}{r_{pL}} + C_8' \quad (2.57)$$

$$y_L' = \frac{4P}{3\pi G r_{pL}^2} \quad (2.58)$$

(3) $a < x < L$

Setting $x = a$ in equations (2.43) and (2.48) (or (2.55) as $r_i = 0$), one obtains y_A and y_A'

$$y_L = y_A + (L - a)y_A' \quad (2.59)$$

$$y_L' = y_A' \quad (2.60)$$

Using the same method discussed in section 2.2.1, one can obtain the displacement of the grid point G by rotation about point L and translation.

2.2.3 Deflection Due to Axial Force

Referring to Fig. 2-7, one can divide the beam into 3 portions for derivation of axial deflections.

$$(1) \quad b < x < c$$

The cross-sectional area of the shaft is

$$A_i = \pi(r_s^2 - r_i^2) \quad (2.61)$$

The deflection along the axis of the shaft is

$$\delta_1 = \frac{P_t(c - b)}{\pi E(r_s^2 - r_i^2)} \quad (2.62)$$

$$(2) \quad a < L < x < b$$

$$r_p = x \tan \theta_p$$

The cross-sectional area of the pitch cone is

$$A_{ii} = \pi(x^2 \tan^2 \theta_p - r_i^2) \quad (2.63)$$

$$\begin{aligned}
d\delta_2 &= \frac{P_t dx}{A_{ii} E} \\
&= \frac{P_t dx}{\pi E (x^2 \tan^2 \theta_p - r_i^2)} \\
\delta_2 &= \frac{P_t}{\pi E \tan^2 \theta_p} \int_L^b \frac{1}{(x^2 - \frac{r_i^2}{\tan^2 \theta_p})} dx \quad (2.64)
\end{aligned}$$

Let

$$A_9 = \frac{P_t}{\pi E \tan^2 \theta_p} \quad (2.65)$$

$$A_7 = \frac{r_i}{\tan \theta_p}$$

If $r_i \neq 0$

$$\begin{aligned}
\delta_2 &= A_9 \int_L^b \left(\frac{1}{x^2 - A_7^2} \right) dx \\
&= \frac{A_9}{2A_7} \ln \left| \frac{(b - A_7)(L + A_7)}{(b + A_7)(L - A_7)} \right| \quad (2.66)
\end{aligned}$$

If $r_i = 0$

$$\begin{aligned}
\delta_2 &= A_9 \int_L^b \frac{dx}{x^2} \\
&= A_9 \left(\frac{1}{L} - \frac{1}{b} \right) \quad (2.67)
\end{aligned}$$

$$(3) \quad a < x < L$$

$$\text{If } r_i \neq 0$$

$$\begin{aligned} \delta_2 &= A_9 \int_a^b \left(\frac{1}{x^2 - A_7^2} \right) dx \\ &= \frac{A_9}{2A_7} \ln \left| \frac{(b - A_7)(a + A_7)}{(b + A_7)(a - A_7)} \right| \end{aligned} \quad (2.68)$$

$$\text{If } r_i = 0$$

$$\begin{aligned} \delta_2 &= A_9 \int_a^b \frac{dx}{x^2} \\ &= A_9 \left(\frac{1}{a} - \frac{1}{b} \right) \end{aligned} \quad (2.69)$$

The displacement of grid point G due to the axial force is

$$\delta = \delta_1 + \delta_2 \quad (2.70)$$

2.2.4 Deflections Due to Torsion

Again, referring to Fig. 2-7, one can divide the beam into 3 portions for derivations of torsional deflections.

$$(1) \quad b < x < e$$

The polar moment of inertia of the shaft is

$$J_1 = \frac{\pi(r_s^4 - r_i^4)}{2} \quad (2.71)$$

The total angle of twist of this portion becomes

$$\begin{aligned} \phi_1 &= \frac{T(e - b)}{GJ_1} \\ &= \frac{2(e - b)T}{\pi G(r_s^4 - r_i^4)} \end{aligned} \quad (2.72)$$

$$(2) \quad a < L < x < b$$

$$r_p = x \tan \theta_p$$

$$J_2 = \frac{\pi(x^4 \tan^4 \theta_p - r_i^4)}{2} \quad (2.73)$$

$$d\phi_2 = \frac{T dx}{GJ_2}$$

$$\begin{aligned} \phi_2 &= \int_L^b \left[\frac{2T}{\pi G(x^4 \tan^4 \theta_p - r_i^4)} \right] dx \\ &= \frac{2T}{\pi G \tan^4 \theta_p} \int_L^b \left(\frac{1}{x^4 - \frac{r_i^4}{\tan^4 \theta_p}} \right) dx \end{aligned} \quad (2.74)$$

Let

$$A_{10} = \frac{2T}{\pi G \tan^4 \theta_p} \quad (2.75)$$

$$A_7 = \frac{r_i}{\tan \theta_p}$$

If $r_i \neq 0$

The total angle of twist of this portion becomes

$$\begin{aligned} \phi_2 &= A_{10} \int_L^b \left(\frac{1}{x^4 - A_7^4} \right) dx \\ &= A_{10} \left[\ln \left(\left| \frac{b - A_7}{L - A_7} \right|^{D_9} \cdot \left| \frac{b + A_7}{L + A_7} \right|^{D_{10}} \right) + \right. \\ &\quad \left. \frac{D_{12}}{A_7} \left(\tan^{-1} \frac{b}{A_7} - \tan^{-1} \frac{L}{A_7} \right) \right] \end{aligned} \quad (2.76)$$

where

$$D_9 = \frac{1}{4A_7^3} \quad (2.77)$$

$$D_{10} = - \frac{1}{4A_7^3} \quad (2.78)$$

$$D_{12} = - \frac{1}{2A_7^2} \quad (2.79)$$

If $r_i = 0$

$$\begin{aligned}
\phi_2 &= A_{10} \int_L^b \frac{dx}{x^4} \\
&= \frac{A_{10}}{3} \left(\frac{1}{L^3} - \frac{1}{b^3} \right)
\end{aligned} \tag{2.80}$$

$$(3) \quad L < x < a$$

$$\text{If } r_i \neq 0$$

$$\begin{aligned}
\phi_2 &= A_{10} \int_a^b \left(\frac{1}{x^4} - \frac{1}{A_7^4} \right) dx \\
&= A_{10} \left[\ln \left(\left| \frac{b - A_7}{a - A_7} \right|^{D_9} \cdot \left| \frac{b + A_7}{a + A_7} \right|^{D_{10}} \right) + \right. \\
&\quad \left. \frac{D_{12}}{A_7} \left(\tan^{-1} \frac{b}{A_7} - \tan^{-1} \frac{a}{A_7} \right) \right]
\end{aligned} \tag{2.81}$$

$$\text{If } r_i = 0$$

$$\begin{aligned}
\phi_2 &= A_{10} \int_a^b \frac{dx}{x^4} \\
&= \frac{A_{10}}{3} \left(\frac{1}{a^3} - \frac{1}{b^3} \right)
\end{aligned} \tag{2.82}$$

ϕ_1 and ϕ_2 can then be added to obtain the total angular displacement of the grid point G.

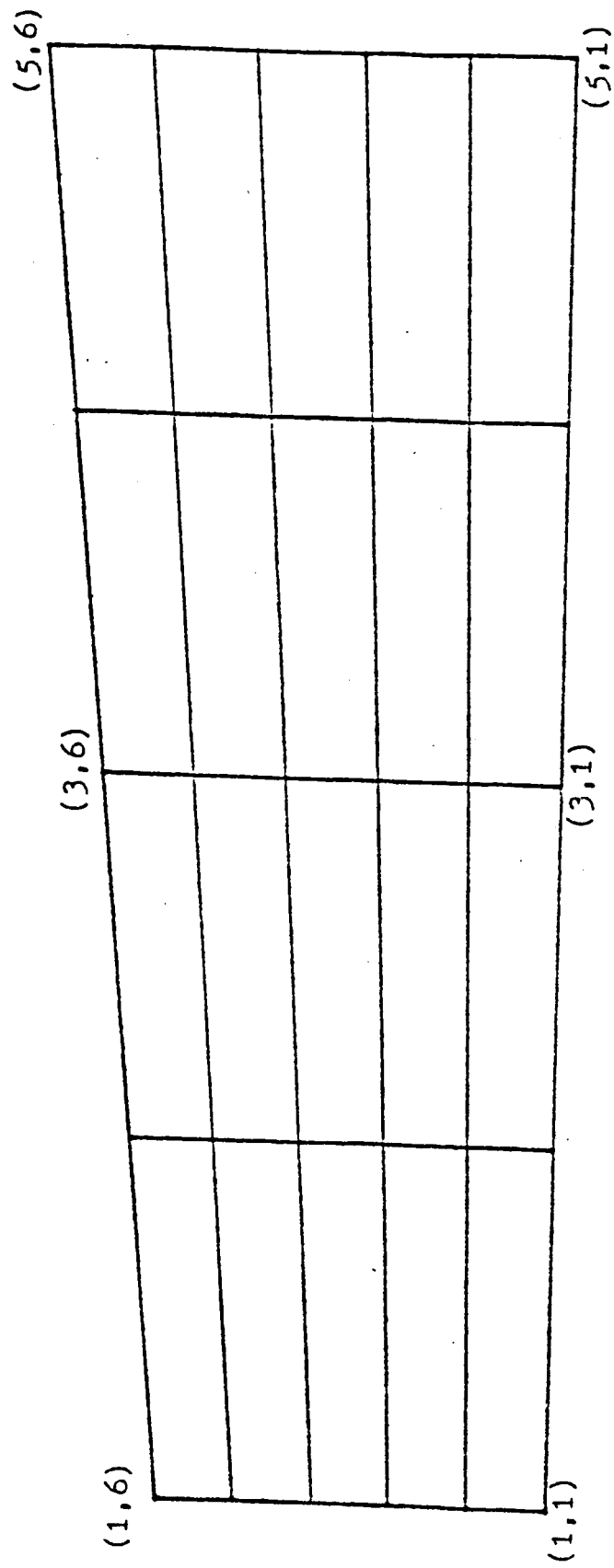


Fig. 2-1 Grid points of a tooth

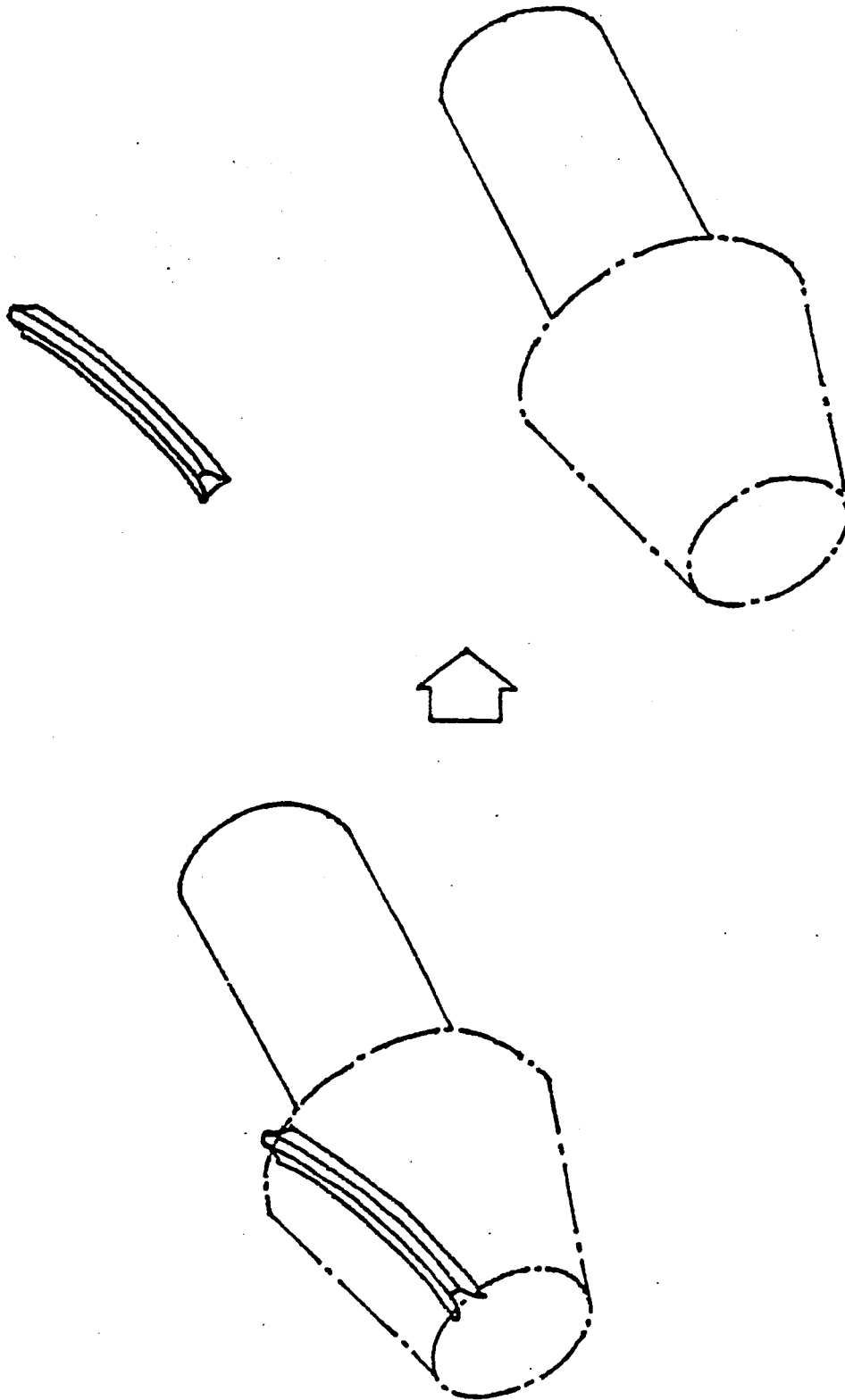


Fig. 2-2 Separation of gear

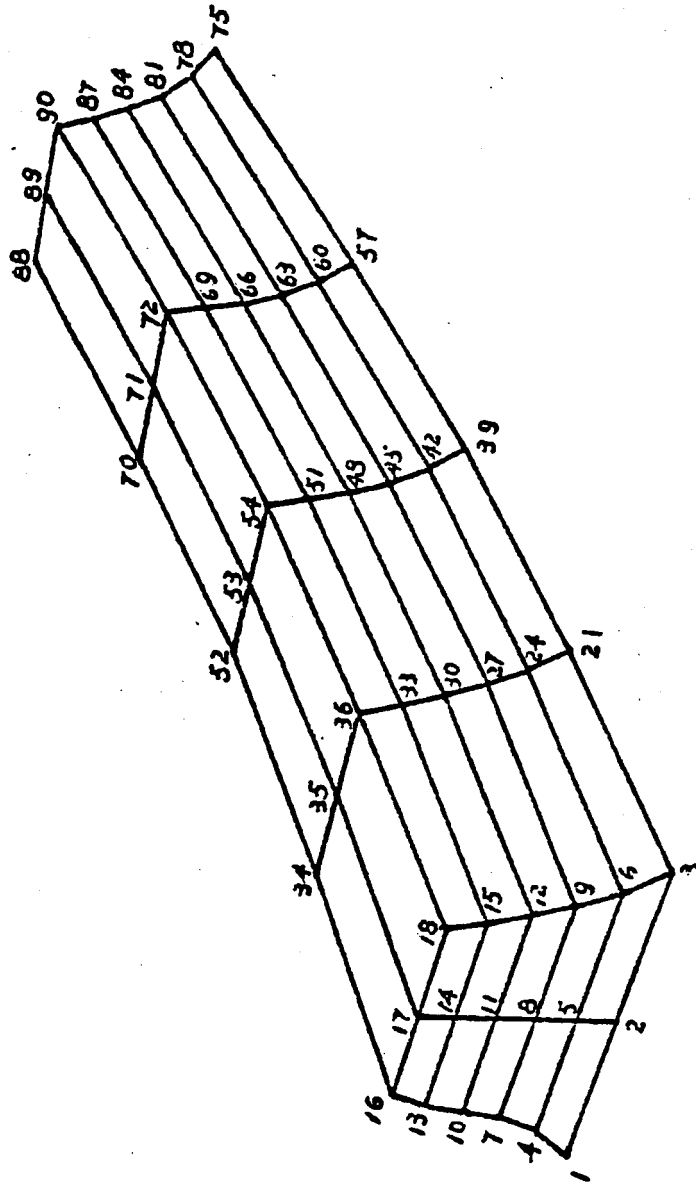


Fig. 2-3 Node number of a tooth

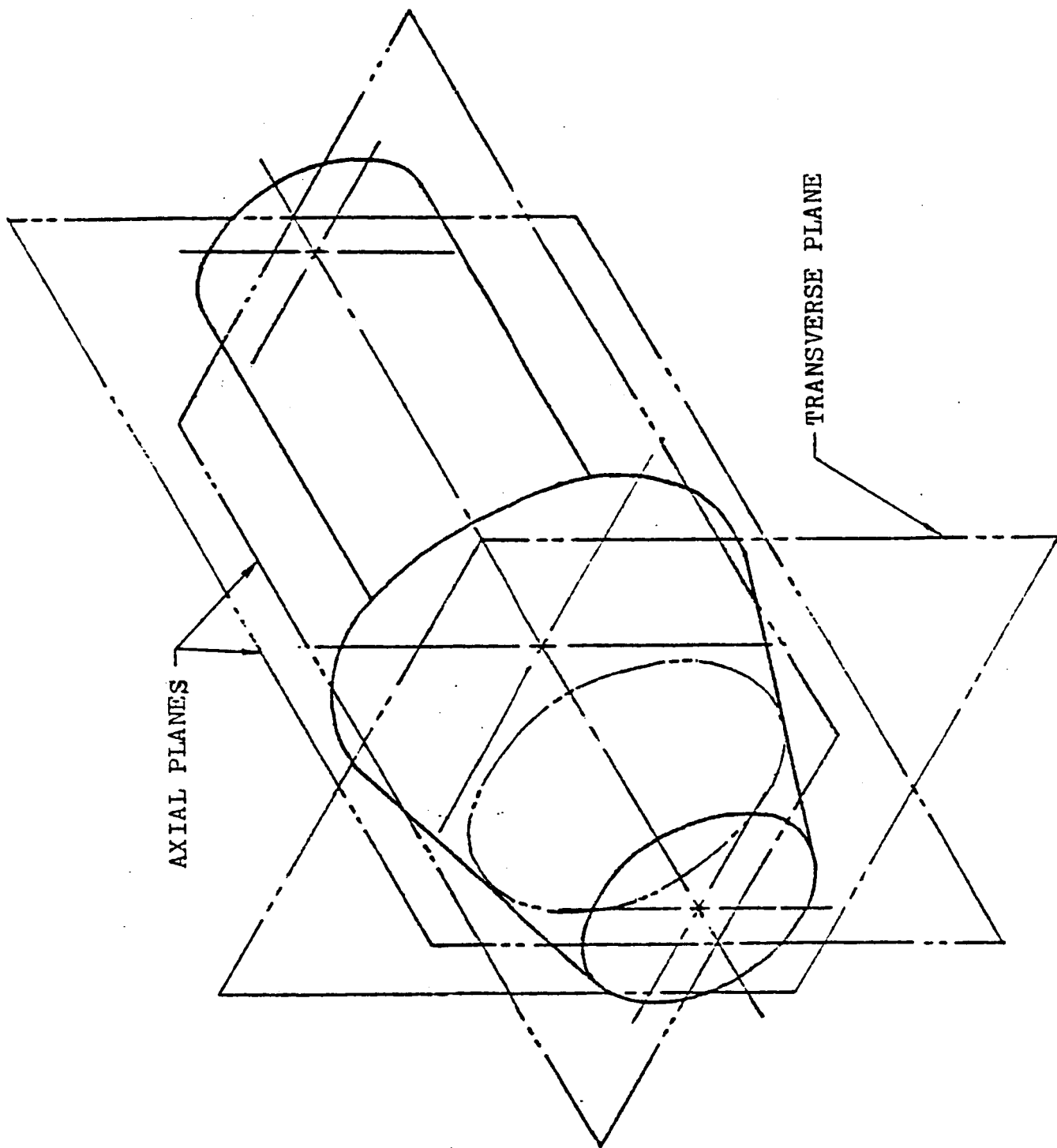


Fig. 2-4 Axial plane and transverse plane

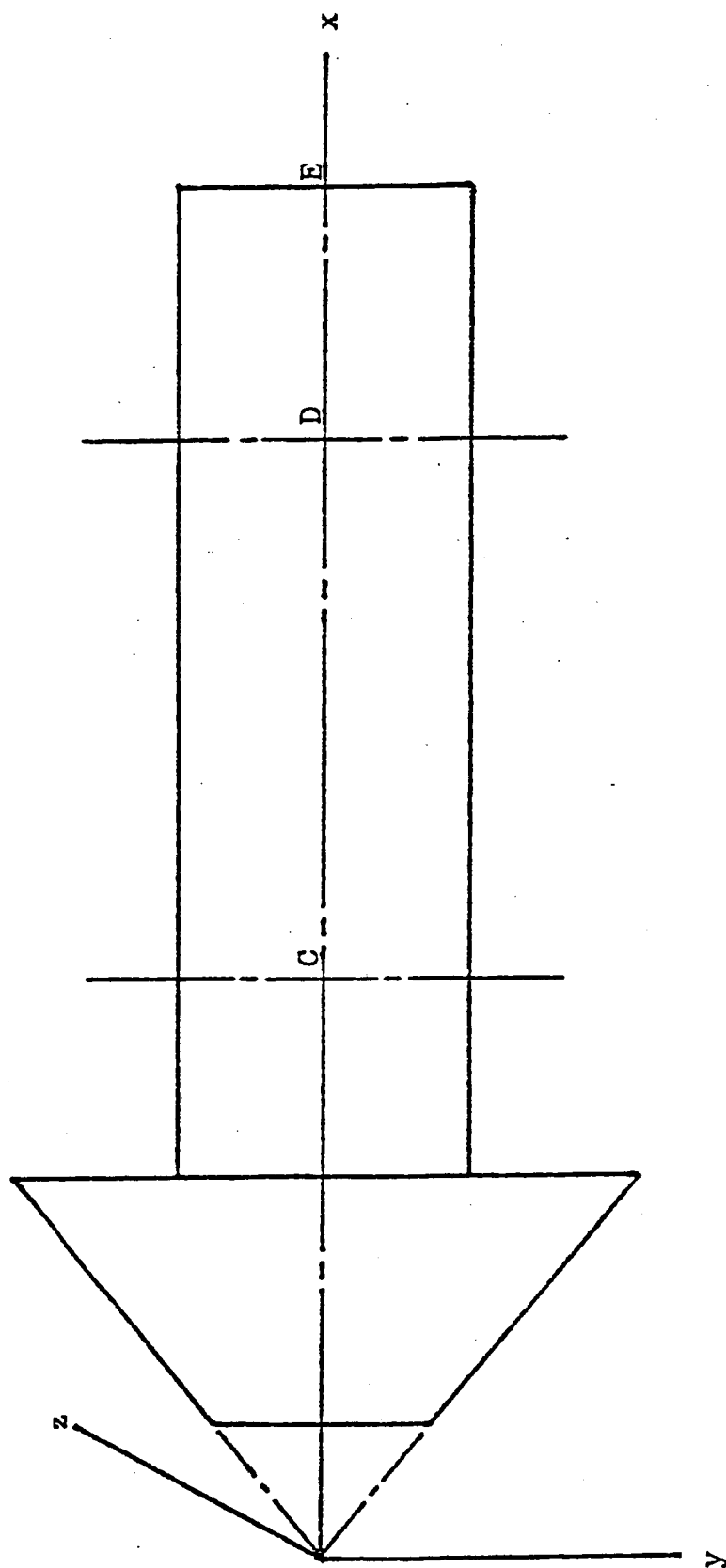


Fig. 2-5 Selection of coordinates for the calculation of deflection of wheel and shaft

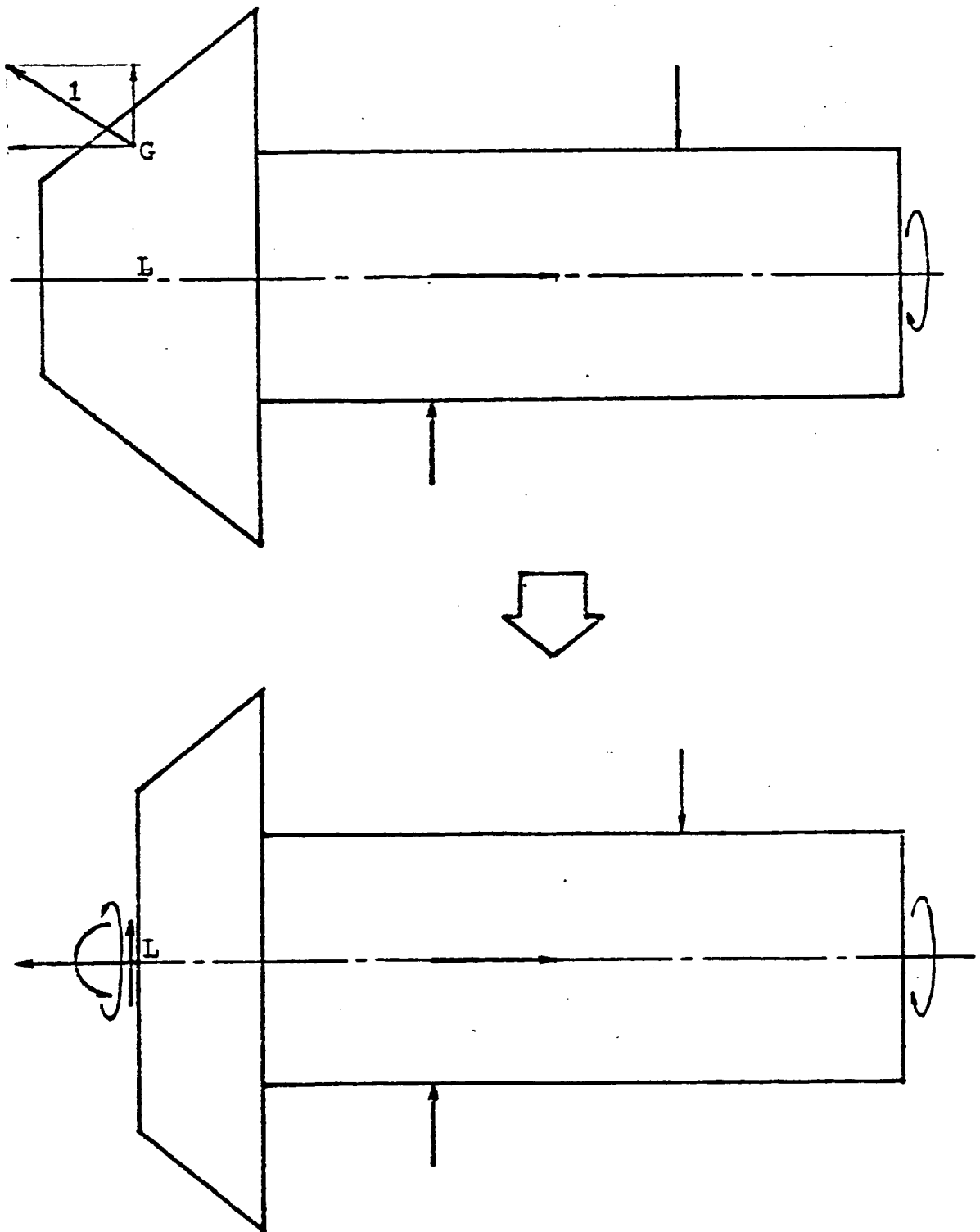


Fig. 2-6 Resolution of the unit normal force
acted on a grid point

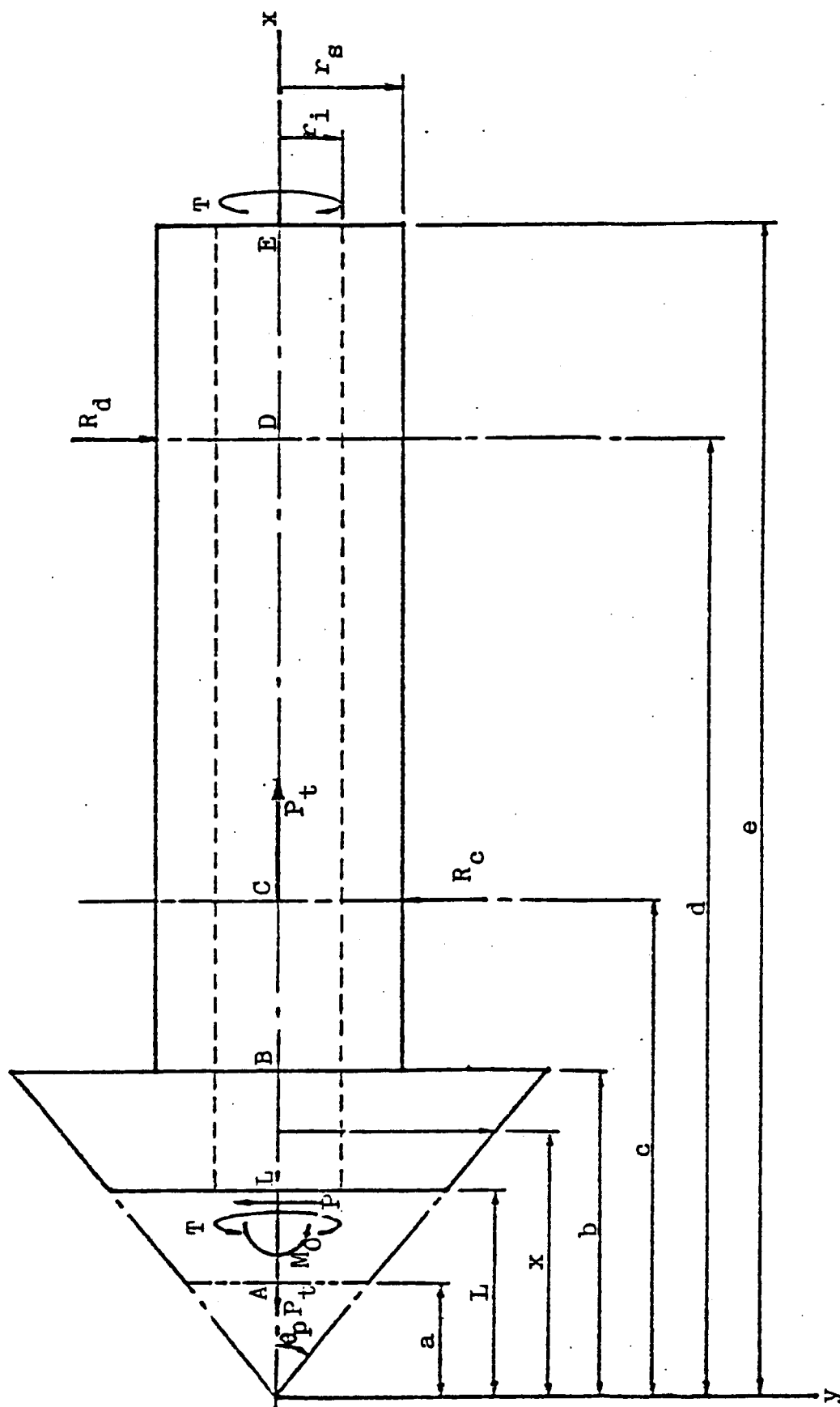


Fig. 2-7 Free body diagram after the resolution of the unit normal force

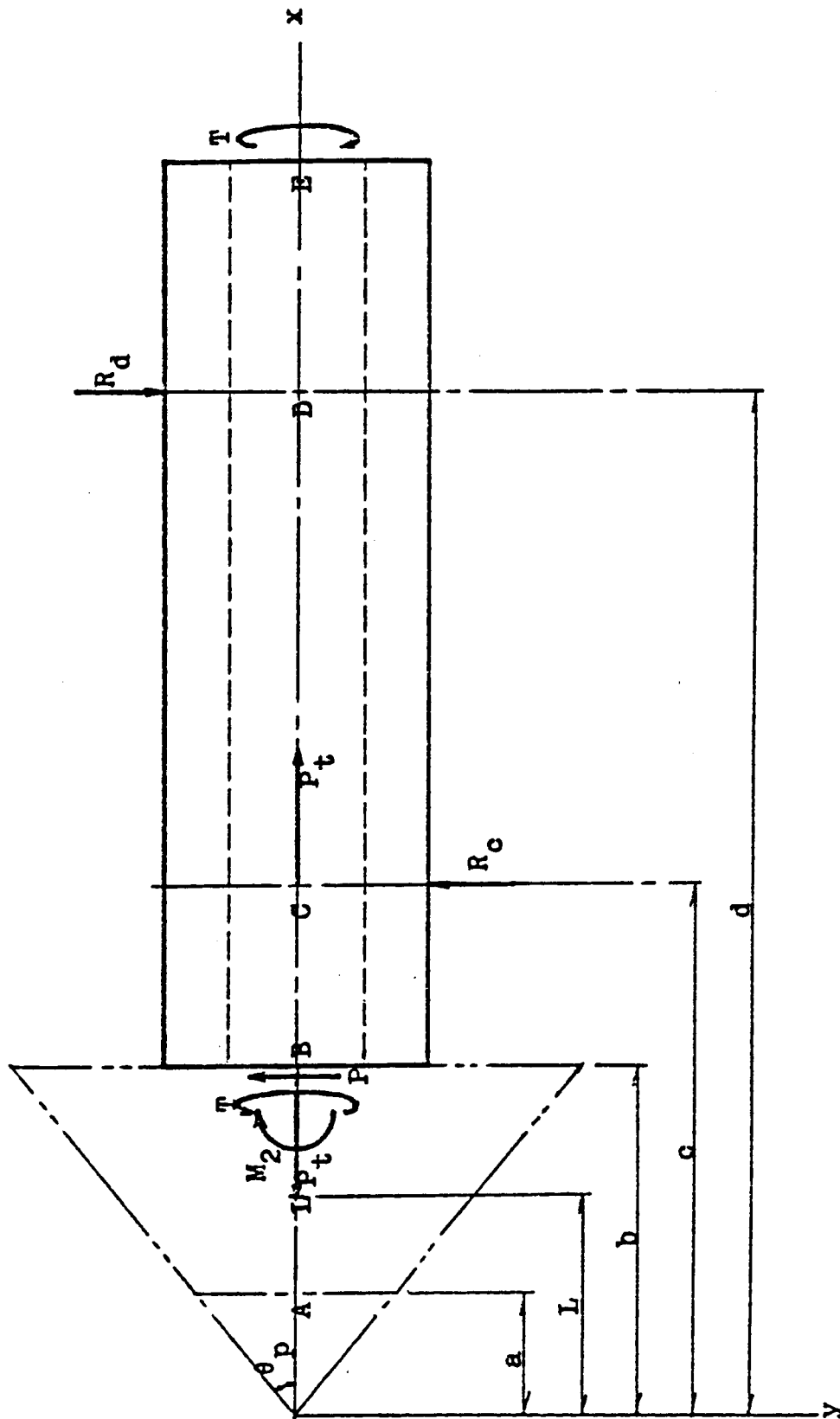


Fig. 2-8 Free body diagram of the beam between the points B and E

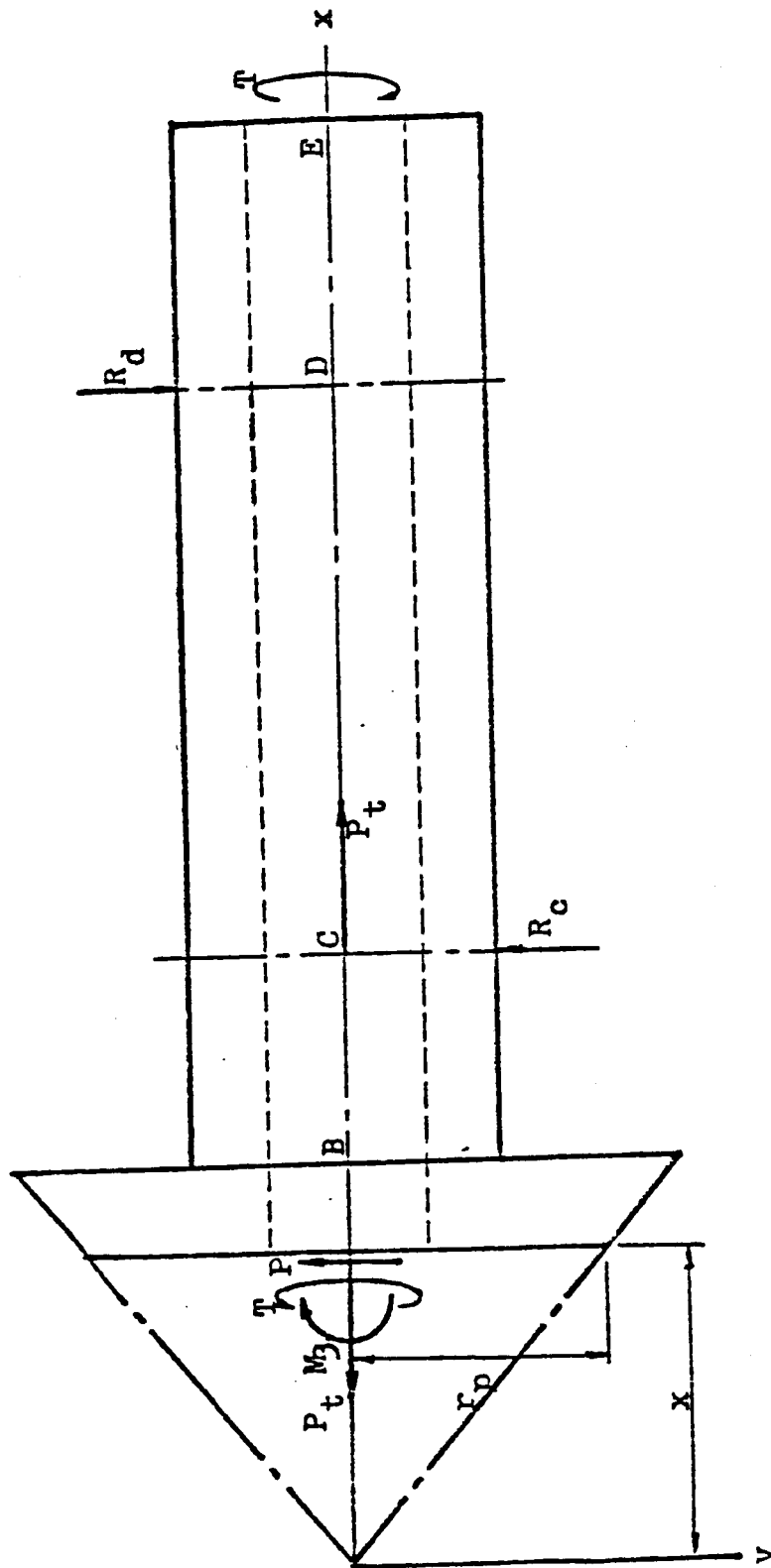


Fig. 2-9 Free body diagram of the beam to the right of point L

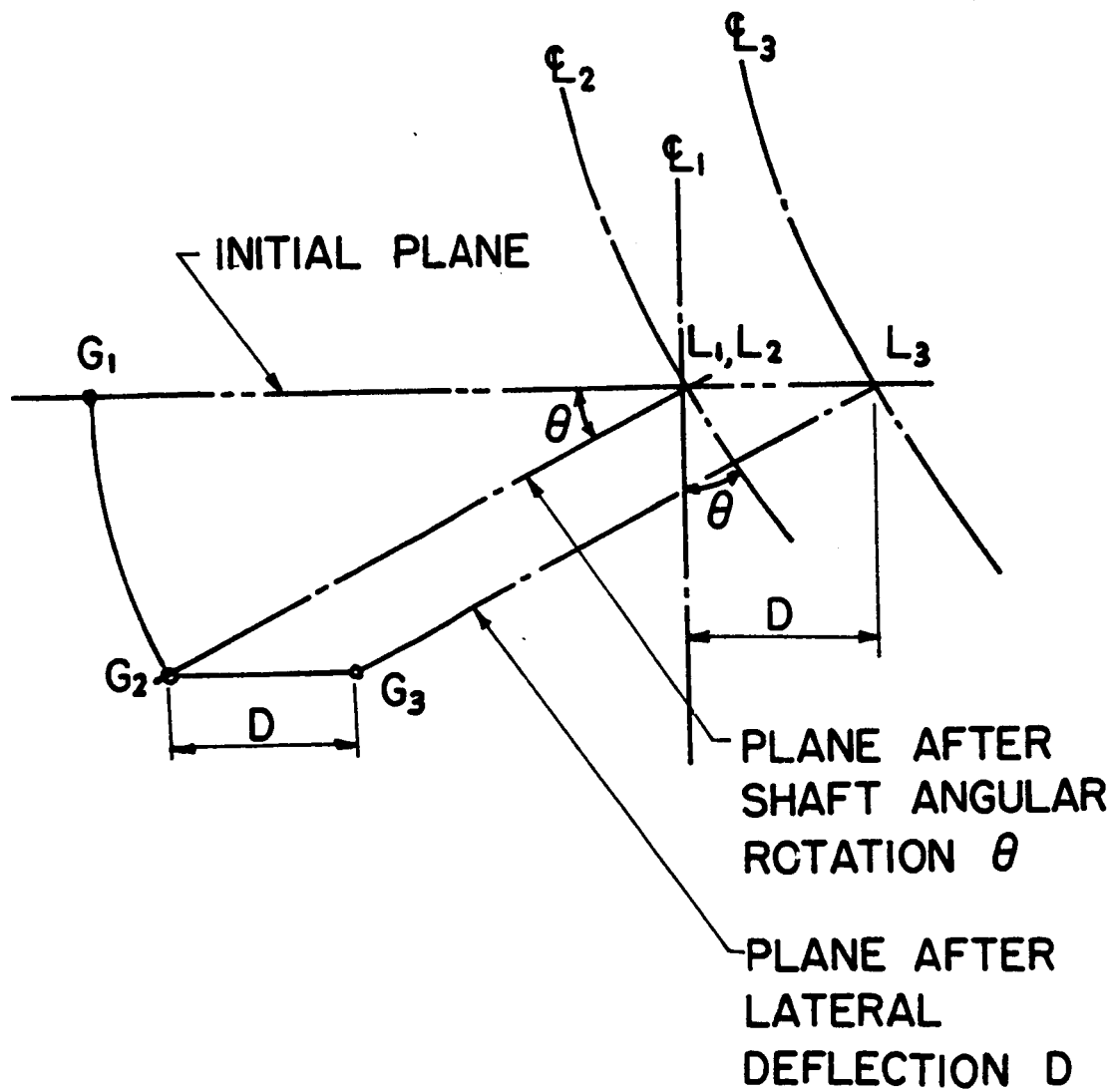


Fig. 2-10. Displacement of the grid point G

CHAPTER III

DISCUSSION OF RESULTS

3.1 Comparison with Charles Chao's Results

Fig. 3-1(p. 35) shows the variation of dynamic load factor(the ratio of the maximum dynamic load along the contact path to the static load at pitch point) as the speed of gear rotation is changed(bearing stiffness = 2,000,000 lbf/in, damping coefficient = 25 lbf.s/in). Since there are 11 degrees of freedom in the spiral bevel gear system, 11 peaks of dynamic load are expected. In the low speed region, a smaller time step in the Runge-Kutta method should be used to facilitate the convergence(Chao used $H = \text{ASTEP}/\text{WG}$ as the time step in Runge-Kutta method, where ASTEP is the rotational angle of the gear between two adjacent contact points used in Runge-Kutta method and WG is the angular speed of the gear).

Compared with Chao's results in Fig. 3-2, one finds that the peaks in Fig. 3-1 shift toward the left side. The reason is that Chao used smaller masses(m), moments of inertia(I) and flexibility influence coefficients(a) in the gear system. From Dunkerley's Formula(11), one finds

$$\omega_n^2 < \text{tr}(\underline{M}^{-1}\underline{K}) \quad (3.1)$$

where ω_n is the largest resonance frequency, tr means

the trace of the following matrix, \underline{M} is the mass matrix and \underline{K} is the stiffness matrix.

When m and I become larger \underline{M}^{-1} becomes smaller. k (element in the stiffness matrix) is the reciprocal of a . So \underline{K} becomes smaller as a becomes larger. In Fig. 3-1, larger m 's, I 's and a 's are used. Then the upper limit of ω_n^2 becomes smaller. This is why the peaks in Fig. 3-1 shift toward the left side.

3.2 Effect of Mass and Moment of Inertia

The upper bound to the resonance frequencies becomes larger when the mass and moment of inertia become smaller. In Fig. 3-3, all the factors are same as those used in Fig. 3-1, except the m and I are smaller. It is seen that the peaks in Fig. 3-3 shift toward the right.

3.3 Effect of Stiffness

The upper bound to the resonance frequencies becomes larger when the stiffness becomes larger. There are two kinds of stiffness in the spiral bevel gear system - contacting stiffness and bearing stiffness. In Fig. 3-4, a larger contacting stiffness was used in comparison to that used in Fig. 3-1. In contrast, a bearing stiffness smaller than that in Fig. 3-1 was used in Fig. 3-5. Expectedly, the peaks in Fig. 3-4 moves toward right due to stiffer teeth, and the peaks in Fig. 3-5 moves toward left due to a softer bearing stiffness.

3.4 Effect of Damping Coefficient

The change of damping coefficient has little influence on the resonance frequency. But the dynamic load increases as the damping coefficient decreases. In Fig. 3-6, a damping coefficient (DC) 15 lbf.s/in was adopted instead of DC = 25 lbf.s/in in Fig. 3-1. It is clearly see that the dynamic load factor in Fig. 3-6 is considerably increased due to a smaller damping coefficient.

(BS20-DC25)

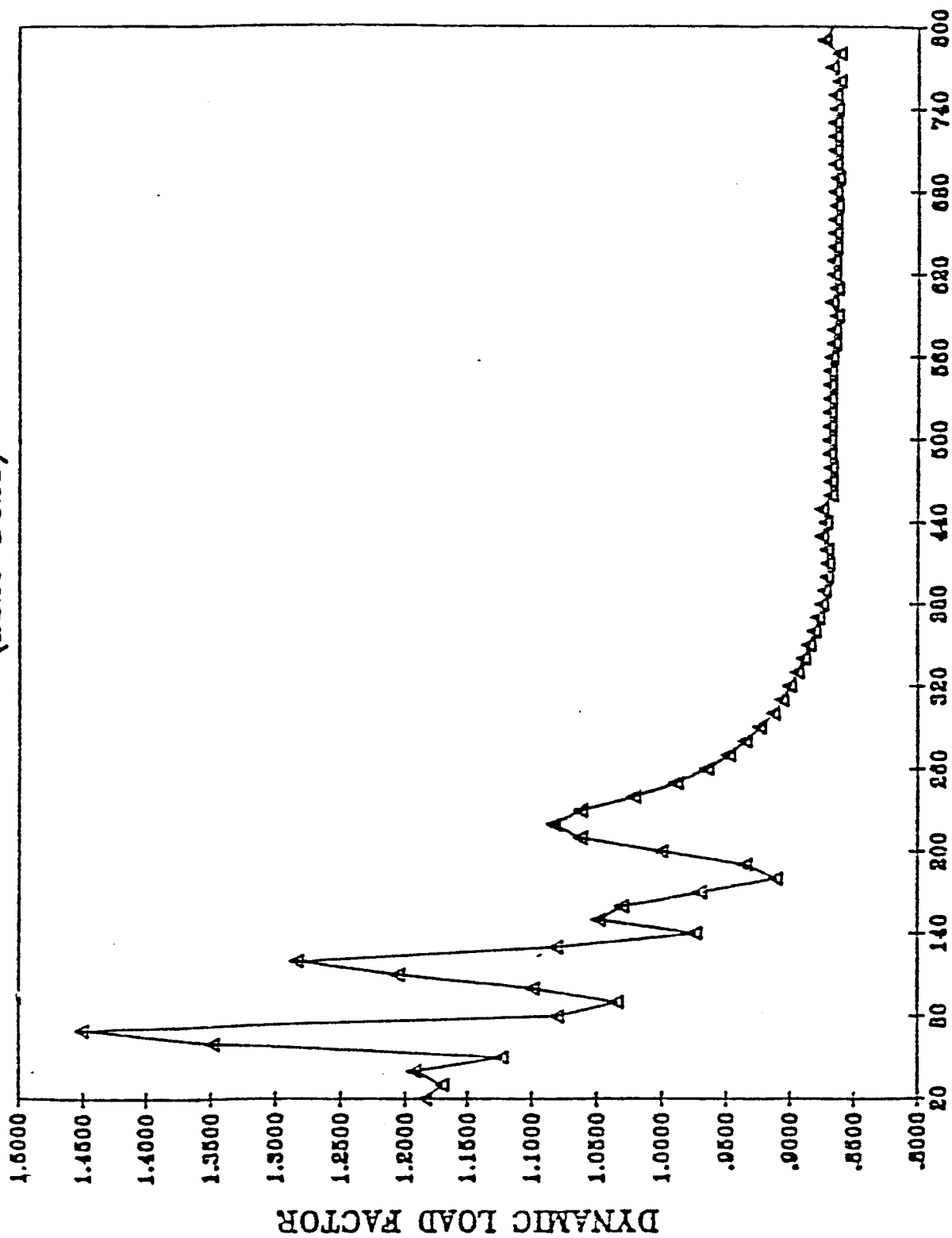


Fig. 3-1 The variation of dynamic load factor as the speed of gear rotation is changed (Hsu's m, I and a, bearing stiffness = 2,000,000 lbf/in, damping coefficient = 25 lbf.s/in)

(BS20-DC25-CMCE)

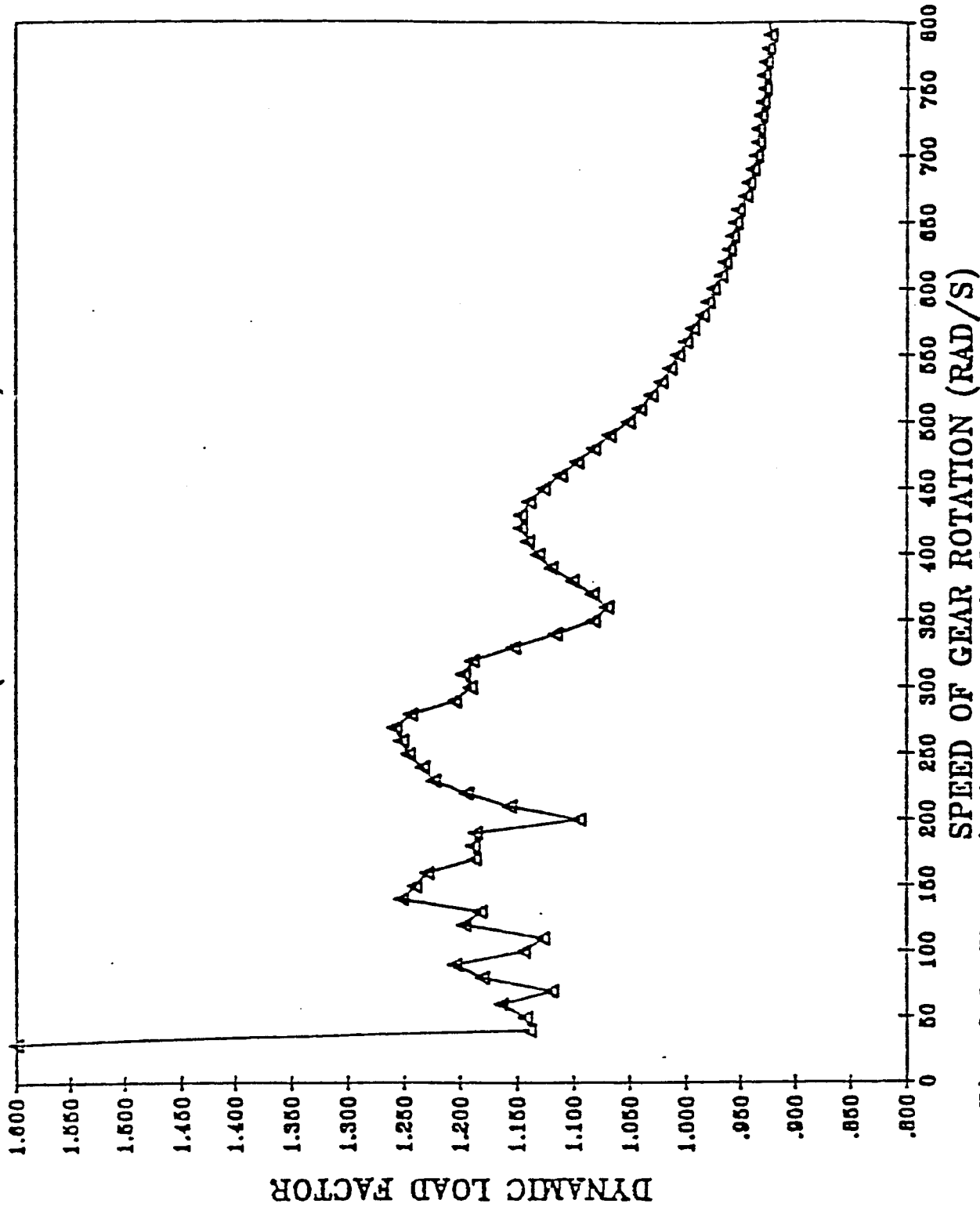


Fig. 3-2 The variation of dynamic load factor as the speed of gear rotation is changed (Chao's m, I and a, bearing stiffness = 2,000,000 lbf/in, damping coefficient = 25 lbf.s/in)

(BS20-DC25-HECM)

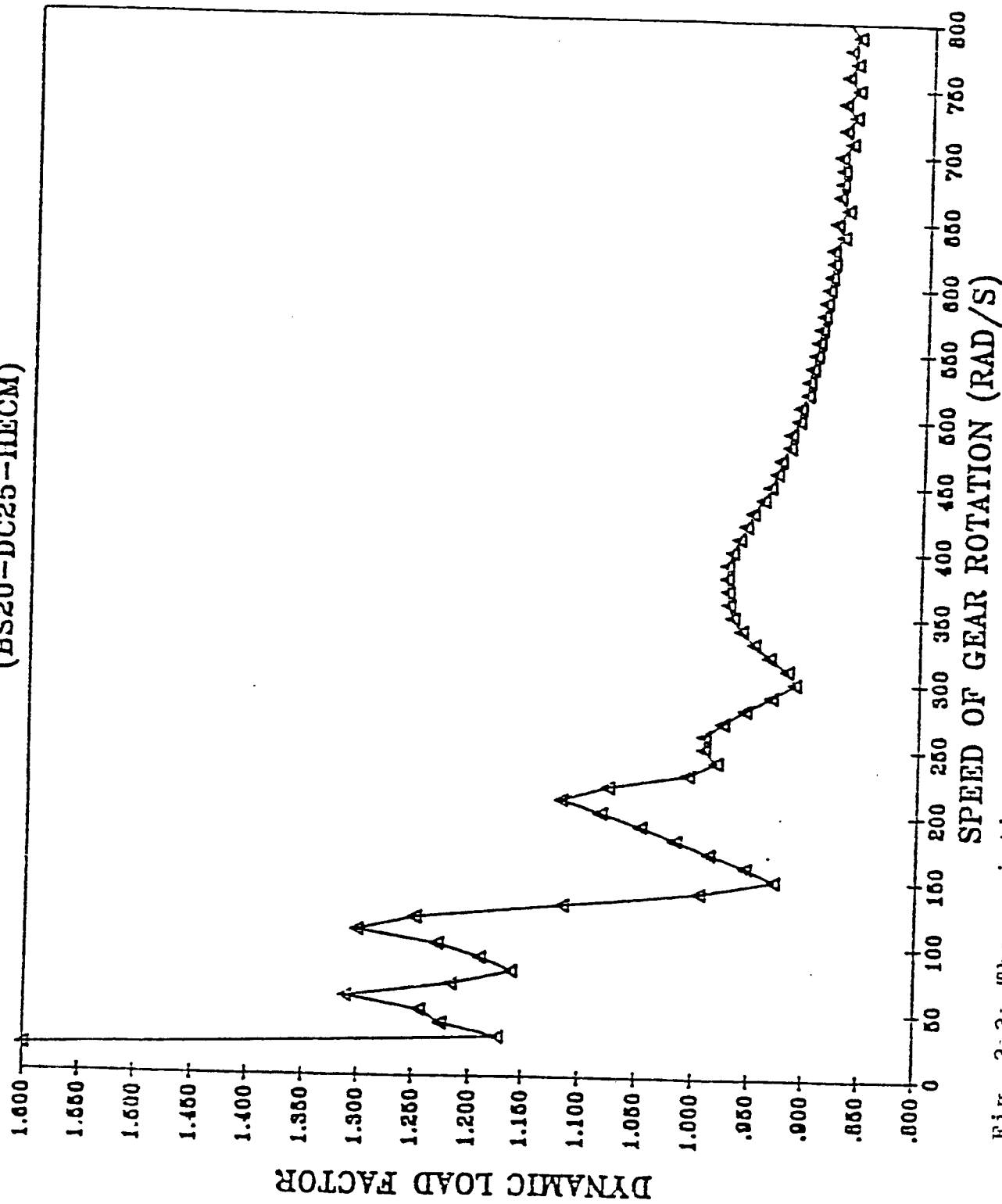


Fig. 3-3 The variation of dynamic load factor as the speed of gear rotation is changed (Chao's m and I, Hsu's a, bearing stiffness = 2,000,000 lbf/in, damping coefficient = 25 lbf.s/in)

(BS20-DC25-HMCE)

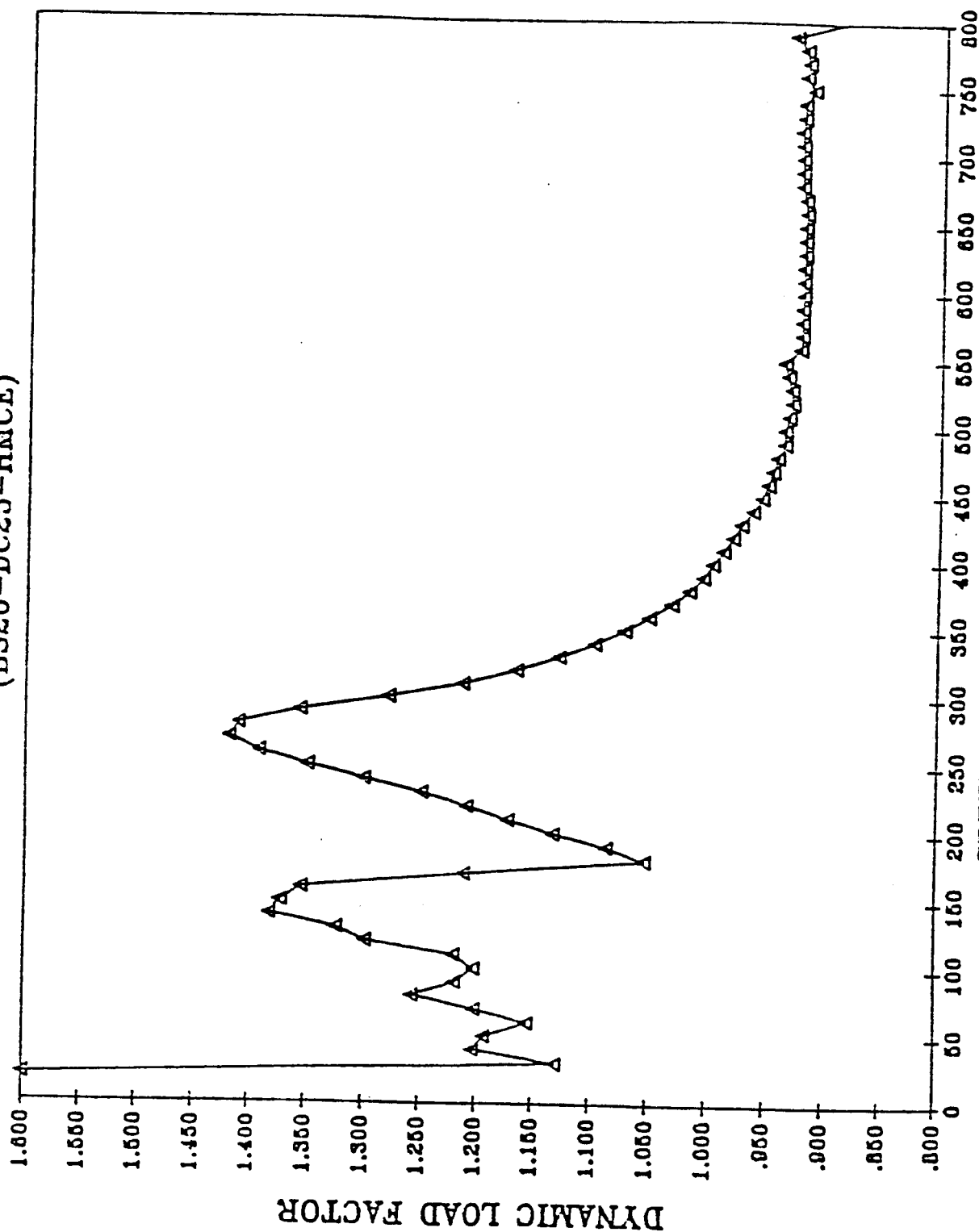


Fig. 3-4 The variation of dynamic load factor as the speed of gear rotation is changed (Hsu's m and I, Chao's a, bearing stiffness = 2,000,000 lbf/in, damping coefficient = 25 lbf.s/in)

(BS10-DC25)

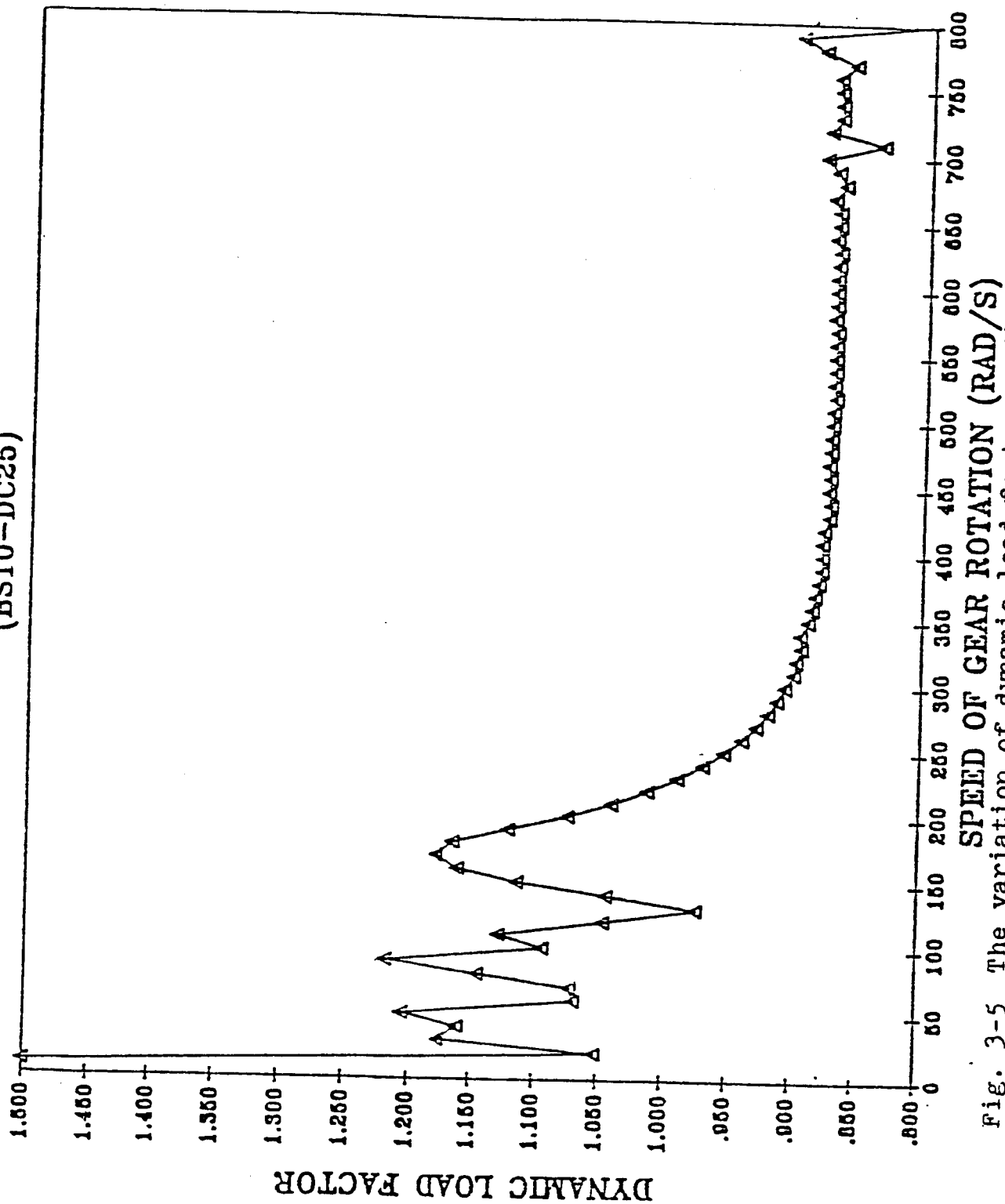


Fig. 3-5 The variation of dynamic load factor as the speed of gear rotation is changed (Hsu's m, I and a, bearing stiffness = 1,000,000 lbf/in, damping coefficient = 25 lbf.s/in)

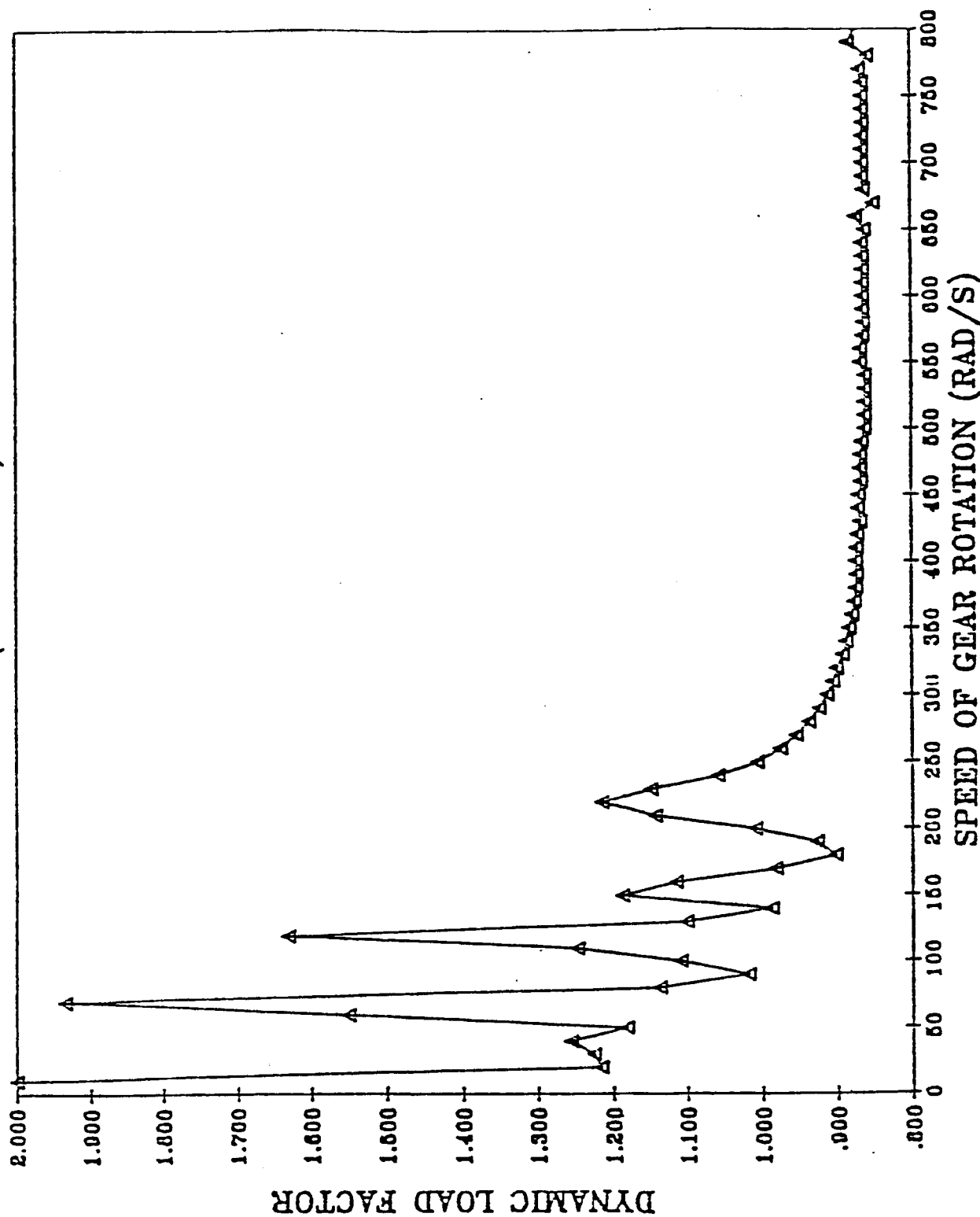


Fig. 3-6 The variation of dynamic load factor as the speed of gear rotation is changed (Hsu's m , I and a , bearing stiffness = 2,000,000 lbf/in, damping coefficient = 15 lbf.s/in)

CHAPTER IV

CONCLUSIONS

A computer code "FLEXM" was developed to calculate the flexibility matrices of contacting teeth for spiral bevel gears using a simplified analysis based on the elementary beam theory for the deformation of gear and shaft. The simplified method requires a computer time at least one order of magnitude less than that needed for the complete FEM(Finite Element Method) Analysis reported earlier by H. C. Chao, and it is much easier to apply for different gear and shaft geometry. Results were obtained for a set of spiral bevel gears whose dimensions are shown in Fig. 4-1. In this case the teeth deflections due to torsion, bending moment, shearing strain and axial force were found to be in the order 10^{-5} , 10^{-6} , 10^{-7} , and 10^{-8} respectively. Thus, for these gears, the torsional deformation is the most predominant part.

In the analysis of dynamic load, resonance frequencies were found to be larger when the mass or moment of inertia is smaller or the stiffness is larger. The change in damping coefficient has little influence on the resonance frequency, but has a marked influence on the dynamic load at the resonant frequencies.

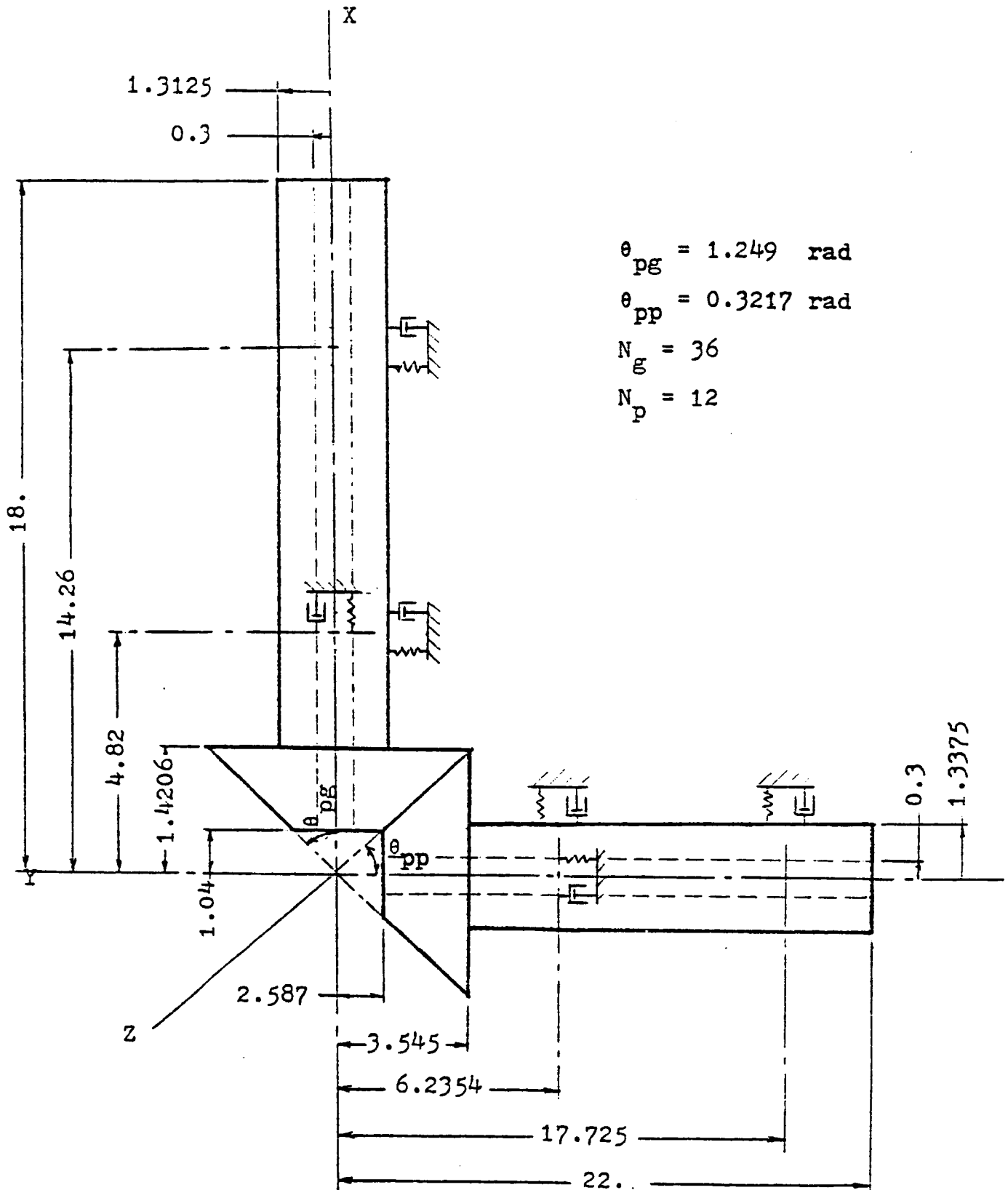


Fig. 4-1 The dimensions for a set of spiral bevel gears

REFERENCES

- (1) Chao, H. C. and Cheng, H. S., "A Computer Solution for the Dynamic Load, Lubricant Film Thickness and Surface Temperatures in Spiral Bevel Gears," NASA CR-4077, 1987.
- (2) Roark, R. J. and Young, W. C., "Formulas for Stress and Strain" McGraw-Hill Book Company, Inc., New York, 1975.
- (3) Chao, H. C., "Tooth Profile and Contact Pattern of Spiral Bevel Gears," M. S. Thesis, Northwestern University, September 1979.
- (4) Chao, H. C., "A Computer Solution for the Dynamic Load, Lubricant Film Thickness and Surface Temperatures in Spiral Bevel Gears," Ph.D. Dissertation, Northwestern University, June 1982.
- (5) Coy, J. J. and Chao, H. C., "A Method of Selecting Grid Size to Account for Hertz Deformation in Finite Element Analysis of Spur Gears," Journal of Mechanical Design, 81-DET-116.
- (6) Wang, K. L. and Cheng, H. S., "A Numerical Solution to the Dynamic Load, Film Thickness, and Surface Temperatures in Spur Gears, Part 1 Analysis," ASME Trans., Journal of Mechanical Design, Volume 103, January 1981, pp. 177-87.
- (7) Wang, K. L. and Cheng, H. S., "A Numerical Solution to the Dynamic Load, Film Thickness, and Surface Temperatures in Spur Gears, Part II-Results," ASME Trans. Journal of Mechanical Design, Volume 103, January 1981, pp. 188-94.

- (8) Bathe, K. J., Wilson, E. L. and Peterson, F. E. "SAP IV : A Structural Analysis Program for Static and Dynamic Response of Linear System," National Science Foundation Contract Report EERC 73-11.
- (9) Timoshenko, S. P. and Young, D. H., "Elements of Strength of Materials," D. Van Nostrand Company, Inc., Princeton, N. J., 1968.
- (10) Budynas, R. G., "Advanced Strength and Applied Stress Analysis," McGraw-Hill Book Company, Inc., 1977.
- (11) Thomson, W. T., "Theory of Vibration with Applications." Prentice-Hall, Inc., Englewood Cliffs, New Jersey, 1981.
- (12) Spotts, M. F., "Design of Machine Elements" Prentice-Hall, Inc., Englewood Cliffs, New Jersey, 1978.
- (13) "AGMA Standard Gear Nomenclature," American Gear Manufacturers Association, AGMA 112. 04, August, 1965.
- (14) Johnson, R. E. and Kiokemeister, F. L., "Calculus," Allyn and Bacon, Inc., Boston, Mass., 1966.
- (15) Gerald, C. F., "Applied Numerical Analysis," Addison-Wesley Publishing Company, Inc., 1978.

NOMENCLATURE

a(in Chapter II)	length along gear (or pinion) axis from the apex of pitch cone to the front plane (refer to Fig. 2-7)
a(in Chapter III)	flexibility influence coefficient
b	length along gear (or pinion) axis from the apex of pitch cone to the back plane (refer to Fig. 2-7)
c	length along gear (or pinion) axis from the apex of pitch cone to the center point of thrust bearing (refer to Fig. 2-7)
DC	damping coefficient
$(D_x)_C$	displacement of point C along x axis
d	length along gear (or pinion) axis from the apex of pitch cone to the center point of radial bearing (refer to Fig. 2-7)
E	modulus of elasticity
e	length along gear (or pinion) axis from the apex of pitch cone to the end plane of shaft (refer to Fig. 2-7)
G	shear modulus
I	moment of inertia
<u>K</u>	stiffness matrix

L	length along gear (or pinion) axis from the apex of pitch cone to the transverse plane through the grid point G (refer to Fig. 2-7)
M	moment
\underline{M}	mass matrix
m	mass
P	shear force
P_t	force along axis of shaft
r_i	radius of hole (refer to Fig. 2-7)
r_p	radius of pitch cone on the cross section passed by transverse plane at a distance x from y axis
r_s	radius of shaft (refer to Fig. 2-7)
T	torque about x axis
y_B	deflection at B in y direction
y'_B	slope at B
δ	deflection along axis of shaft
θ_p	pitch angle
$(\theta_x)_E$	angular displacement about x axis at point E
ϕ	twist angle about x axis

τ_{\max}

maximum shear stress

ω_n

the largest resonance frequency

APPENDIX A

TWO SAMPLES OF INPUT DATA FOR SAPIV

```

123456789 123456789 123456789 123456789 123456789 123456789 123456789 1234
56789
10 VCHANG,CHUF5341-9079,CM300000,T500,PO.
20 PASSWORD
30 ATTACH,A,HSUSAP4-BI.
40 A.
50 CATALOG,TAPE20,HSUSAP4-GEAR-OUTFLEX,RP=999.
60 EOR
70 GEAR(5X6)
80 90 1 50
90 1 1 1 1 1 1 1 1.0399854-2.4486161 .4517907
70.000
100 2 1 1 1 1 1 1 1.0400479-2.4734411 .2859099
70.000
110 3 1 1 1 1 1 1 1.0401105-2.4870416 .1187368
70.000
120 4 .9896887-2.4691688 .4321978
70.000
130 5 .9897411-2.4902692 .2863700
70.000
140 6 .9897934-2.5027648 .1395562
70.000
(S,C OR RETURN)>
123456789 123456789 123456789 123456789 123456789 123456789 123456789 1234
56789
150 7 .9393643-2.4897020 .4115088
70.000
160 8 .9394231-2.5070557 .2872147
70.000
170 9 .9394819-2.5182082 .1622131
70.000
180 10 .8890503-2.5101851 .3896827
70.000
190 11 .8891085-2.5238156 .2882939
70.000
200 12 .8891667-2.5333526 .1864398
70.000
210 13 .8387271-2.5305982 .3666830
70.000
220 14 .8387884-2.5405633 .2895019
70.000
230 15 .8388497-2.5481750 .2120541
70.000
240 16 .7884157-2.5509090 .3425093
70.000
(S,C OR RETURN)>

```

	123456789	123456789	123456789	123456789	123456789	123456789	123456789	1234
250	17							.7884783-2.5573020 .2907752
	70.000							
260	18							.7885409-2.5626458 .2389230
	70.000							
270	19	1	1	1	1	1	1	1.1352225-2.6996818 .3451271
	70.000							
280	20	1	1	1	1	1	1	1.1352028-2.7170012 .1592737
	70.000							
290	21	1	1	1	1	1	1	1.1351831-2.7215411 -.0273304
	70.000							
300	22							1.0803056-2.7203453 .3218651
	70.000							
310	23							1.0802674-2.7352711 .1589196
	70.000							
320	24							1.0802293-2.7399470 -.0046002
	70.000							
330	25							1.0255804-2.7421413 .2973606
	70.000							
340	26							1.0255730-2.7536389 .1588615
	70.000							

(S,C OR RETURN)>

	123456789	123456789	123456789	123456789	123456789	123456789	123456789	1234
350	27							1.0255656-2.7581457 .0199593
	70.000							
360	28							.9708458-2.7631816 .2717251
	70.000							
370	29							.9708263-2.7719840 .1591097
	70.000							
380	30							.9708069-2.7761985 .0462282
	70.000							
390	31							.9158890-2.7839132 .2448944
	70.000							
400	32							.9159172-2.7901563 .1595966
	70.000							
410	33							.9159454-2.7937865 .0741464
	70.000							
420	34							.8611402-2.8046768 .2167437
	70.000							
430	35							.8611331-2.8084820 .1600917
	70.000							
440	36							.8611260-2.8111431 .1033747
	70.000							

(S,C OR RETURN)>

	123456789	123456789	123456789	123456789	123456789	123456789	123456789	1234
56739								
450 37	1	1	1	1	1	1	1.2303581-2.9460965	.2087316
70.000								
460 38	1	1	1	1	1	1	1.2303544-2.9534790	.0035044
70.000								
470 39	1	1	1	1	1	1	1.2303507-2.9465825	-.2017395
70.000								
480 40							1.1710455-2.9677205	.1813078
70.000								
490 41							1.1710277-2.9732519	.0020571
70.000								
500 42							1.1710100-2.9679665	-.1772007
70.000								
510 43							1.1116919-2.9891879	.1526480
70.000								
520 44							1.1117126-2.9930541	.0010429
70.000								
530 45							1.1117332-2.9892363	-.1505618
70.000								
540 46							1.0524332-3.0102897	.1228540
70.000								
(S,C OR RETURN)>								
	123456789	123456789	123456789	123456789	123456789	123456789	123456789	1234
56789								
550 47							1.0524284-3.0127978	.0003868
70.000								
560 48							1.0524236-3.0103257	-.1220810
70.000								
570 49							.9932511-3.0312032	.0917458
70.000								
580 50							.9932042-3.0325977	-.0001401
70.000								
590 51							.9931573-3.0312075	-.0920260
70.000								
600 52							.9338390-3.0518240	.0593035
70.000								
610 53							.9338223-3.0523730	-.0005446
70.000								
620 54							.9338057-3.0517485	-.0603912
70.000								
630 55	1	1	1	1	1	1	1.3255356-3.1849165	.0410155
70.000								
640 56	1	1	1	1	1	1	1.3254829-3.1799661	-.1827477
70.000								
(S,C OR RETURN)>								

	123456789	123456789	123456789	123456789	123456789	123456789	123456789	1234
56789								
650	57	1	1	1	1	1	1	1.3254301-3.1593141 -.4056129
	70.000							
660	58							1.2617374-3.2064396 .0090159
	70.000							
670	59							1.2616901-3.2011132 -.1854066
	70.000							
680	60							1.2616427-3.1840088 -.3791497
	70.000							
690	61							1.1979185-3.2276346 -.0242081
	70.000							
700	62							1.1978853-3.2222936 -.1875536
	70.000							
710	63							1.1978521-3.2086911 -.3504202
	70.000							
720	64							1.1341340-3.2484637 -.0587046
	70.000							
730	65							1.1341174-3.2434813 -.1893942
	70.000							
740	66							1.1341007-3.2332433 -.3197775
	70.000							
(S,C OR RETURN)>								
	123456789	123456789	123456789	123456789	123456789	123456789	123456789	1234
	56789							
750	67							1.0703415-3.2688987 -.0945045
	70.000							
760	68							1.0702406-3.2647258 -.1909900
	70.000							
770	69							1.0701397-3.2577056 -.2873113
	70.000							
780	70							1.0065434-3.2889042 -.1315752
	70.000							
790	71							1.0065002-3.2859255 -.1925140
	70.000							
800	72							1.0064570-3.2818173 -.2533874
	70.000							
810	73	1	1	1	1	1	1	1.4206645-3.4131983 -.1603038
	70.000							
820	74	1	1	1	1	1	1	1.4206129-3.3933350 -.4014192
	70.000							
830	75	1	1	1	1	1	1	1.4205613-3.3564603 -.6405270
	70.000							
840	76							1.3523712-3.4340588 -.1974156
	70.000							
(S,C OR RETURN)>								

```

123456789 123456789 123456789 123456789 123456789 123456789 123456789 1234
56789
850 77 1.3523284-3.4157766 -.4054566
70.000
860 78 1.3522856-3.3849026 -.6120060
70.000
870 79 1.2840544-3.4544599 -.2357822
70.000
880 80 1.2840289-3.4382864 -.4089625
70.000
890 81 1.2840034-3.4134364 -.5811130
70.000
900 82 1.2157806-3.4743604 -.2754484
70.000
910 83 1.2157640-3.4608747 -.4121853
70.000
920 84 1.2157474-3.4420097 -.5482869
70.000
930 85 1.1474946-3.4937288 -.3164317
70.000
940 86 1.1474580-3.4834143 -.4151088
70.000
(S,C OR RETURN)>
123456789 123456789 123456789 123456789 123456789 123456789 123456789 1234
56789
950 87 1.1474214-3.4703133 -.5134553
70.000
960 88 1.0792083-3.5125335 -.3586650
70.000
970 89 1.0791680-3.5060147 -.4178961
70.000
980 90 1.0791277-3.4984971 -.4770090
70.000
990 5 40 1
1000 1 30000000. .3 .283 .0000073
1010 386.
1020
1030
1040
1050
1060
1070 1 1 2 20 19 4 5 23 22 2 1 3
70.
1080 5 13 14 32 31 16 17 35 34 2 1
70.
(S,C OR RETURN)>

```


123456789 123456789 123456789 123456789 123456789 123456789 123456789 1234
56789

1350	25	13	.1922	.5016	-.8435
1360	27	14	-.4881	.3509	-.7992
1370	28	15	.2050	.5106	-.8350
1380	30	16	-.5035	.3402	-.7942
1390	31	17	.2178	.5191	-.8265
1400	33	18	-.5170	.3307	-.7895
1410	34	19	.2307	.5273	-.8178
1420	36	20	-.5290	.3222	-.7851
1430	40	21	.1687	.5761	-.7998
1440	42	22	-.4850	.4384	-.7567
1450	43	23	.1796	.5852	-.7908
1460	45	24	-.5024	.4252	-.7529
1470	46	25	.1911	.5940	-.7815
1480	48	26	-.5168	.4139	-.7494
1490	49	27	.2027	.6024	-.7720
1500	51	28	-.5293	.4040	-.7461
1510	52	29	.2143	.6104	-.7626
1520	54	30	-.5405	.3948	-.7429
1530	58	31	.1569	.6570	-.7374
1540	60	32	-.5008	.5096	-.6996

(S,C OR RETURN)>

123456789 123456789 123456789 123456789 123456789 123456789 123456789 1234
56789

1550	61	33	.1666	.6658	-.7273
1560	63	34	-.5169	.4961	-.6977
1570	64	35	.1769	.6744	-.7169
1580	66	36	-.5301	.4844	-.6959
1590	67	37	.1872	.6826	-.7065
1600	69	38	-.5417	.4740	-.6942
1610	70	39	.1972	.6903	-.6961
1620	72	40	-.5521	.4644	-.6925
1630	76	41	.1449	.7338	-.6637
1640	78	42	-.5168	.5763	-.6331
1650	79	43	.1535	.7424	-.6522
1660	81	44	-.5314	.5627	-.6332
1670	82	45	.1624	.7506	-.6405
1680	84	46	-.5435	.5509	-.6334
1690	85	47	.1713	.7585	-.6288
1700	87	48	-.5540	.5401	-.6335
1710	88	49	.1795	.7660	-.6173
1720	90	50	-.5637	.5300	-.6335

1730

1740

(S,C OR RETURN)>

123456789 123456789 123456789 123456789 123456789 123456789 123456789 1234
56789

1750
1760
1770
1780
1790
1800
1810
1820
1830
1840
1850
1860
1870
1880
1890
1900
1910
1920
1930
1940

(S,C OR RETURN)>

123456789 123456789 123456789 123456789 123456789 123456789 123456789 1234
56789

1950
1960
1970
1980
1990
2000
2010
2020
2030
2040
2050
2060
2070
2080
2090
2100
2110
2120
2130
2140

(S,C OR RETURN)>

123456789 123456789 123456789 123456789 123456789 123456789 1234
56789

2150

2160

2170

2180

2190

2200

2210

2220

2230

2240

2250

2260 EOI

>

```

123456789 123456789 123456789 123456789 123456789 123456789 123456789 1234
56789
10 VCHANG,CHUF5341-9079,CM300000,T500,PO.
20 PASSWORD
30 ATTACH,A,HSUSAP4-BI.
40 A.
50 CATALOG,TAPE20,HSUSAP4-PINION-OUTFLEX,RP=999.
60 EOR
70 PINION(5X6)
80 90 1 50
90 1 1 1 1 1 1 1 .7493591-2.5867077 .0961353
70.000
100 2 1 1 1 1 1 1 .7105503-2.5867380 .2547510
70.000
110 3 1 1 1 1 1 1 .6396983-2.5867683 :4025284
70.000
120 4 .7950604-2.5697191 .1267436
70.000
130 5 .7586351-2.5697031 .2695487
70.000
140 6 .6967888-2.5696870 .4033212
70.000
(S,C OR RETURN)>
123456789 123456789 123456789 123456789 123456789 123456789 123456789 1234
56789
150 7 .8406950-2.5527553 .1573071
70.000
160 8 .8067394-2.5526930 .2840528
70.000
170 9 .7537959-2.5526307 .4041128
70.000
180 10 .8836706-2.5356435 .1971727
70.000
190 11 .8546212-2.5356184 .2988727
70.000
200 12 .8139109-2.5355884 .3964881
70.000
210 13 .9236519-2.5185588 .2447413
70.000
220 14 .9026101-2.5185250 .3135165
70.000
230 15 .8764554-2.5184911 .3805130
70.000
240 16 .9601221-2.5014674 .2991586
70.000
(S,C OR RETURN)>

```

	123456789	123456789	123456789	123456789	123456789	123456789	123456789	1234
56789								
250 17								.9507147-2.5014348 .3277974
70.000								
260 18								.9404533-2.5014022 .3561410
70.000								
270 19	1	1	1	1	1	1	1	.8276093-2.8262767 -.0357977
70.000								
280 20	1	1	1	1	1	1	1	.8148691-2.8262729 .1444194
70.000								
290 21	1	1	1	1	1	1	1	.7648936-2.8262690 .3186656
70.000								
300 22								.3821774-2.8076628 -.0104465
70.000								
310 23								.8690964-2.8076599 .1515968
70.000								
320 24								.8265055-2.8076571 .3084850
70.000								
330 25								.9366826-2.7890703 .0148756
70.000								
340 26								.9233059-2.7890684 .1584728
70.000								
(S,C OR RETURN)>								
123456789	123456789	123456789	123456789	123456789	123456789	123456789	123456789	1234
56789								
350 27								.8880466-2.7890665 .2983160
70.000								
360 28								.9903133-2.7705973 .0504391
70.000								
370 29								.9775167-2.7705719 .1656822
70.000								
380 30								.9513575-2.7705465 .2786274
70.000								
390 31								1.0418918-2.7519397 .0948586
70.000								
400 32								1.0317557-2.7519091 .1726900
70.000								
410 33								1.0158144-2.7518785 .2495356
70.000								
420 34								1.0907050-2.7333002 .1470639
70.000								
430 35								1.0859416-2.7332657 .1791881
70.000								
440 36								1.0802322-2.7332312 .2111591
70.000								
(S,C OR RETURN)>								

	123456789	123456789	123456789	123456789	123456789	123456789	123456789	1234
450	37	1	1	1	1	1	1	.8800131-3.0656536 -.1932156
	70.000							
460	38	1	1	1	1	1	1	.9001061-3.0657021 .0036763
	70.000							
470	39	1	1	1	1	1	1	.8786765-3.0657506 .2010801
	70.000							
480	40							.9431940-3.0456198 -.1753063
	70.000							
490	41							.9593132-3.0456258 .0013620
	70.000							
500	42							.9426273-3.0456318 .1779714
	70.000							
510	43							1.0063188-3.0256037 -.1574129
	70.000							
520	44							1.0184613-3.0255673 -.0012654
	70.000							
530	45							1.0065213-3.0255309 .1548833
	70.000							
540	46							1.0700859-3.0052346 -.1281752
	70.000							

(S,C OR RETURN)>

	123456789	123456789	123456789	123456789	123456789	123456789	123456789	1234
550	47							1.0776598-3.0053157 -.0034644
	70.000							
560	48							1.0707496-3.0053967 .1212768
	70.000							
570	49							1.1333126-2.9852888 -.0896833
	70.000							
580	50							1.1367420-2.9852550 -.0060019
	70.000							
590	51							1.1340015-2.9852211 .0776976
	70.000							
600	52							1.1952105-2.9650718 -.0420047
	70.000							
610	53							1.1958550-2.9650548 -.0089431
	70.000							
620	54							1.1955852-2.9650379 .0241219
	70.000							
630	55	1	1	1	1	1	1	.8995507-3.3051870 -.3725657
	70.000							
640	56	1	1	1	1	1	1	.9584656-3.3051394 -.1655958
	70.000							

(S,C OR RETURN)>

	1234	56789	1234	56789	1234	56789	1234	56789	1234	56789	1234	56789	1234	56789	1234
650	57	1	1	1	1	1	1	.9728761-3.3050918	.0498089						
	70.000														
660	58							.9703256-3.2835967	-.3641763						
	70.000														
670	59							1.0208089-3.2835200	-.1791273						
	70.000														
680	60							1.0363269-3.2834433	.0120539						
	70.000														
690	61							1.0410536-3.2620206	-.3557925						
	70.000														
700	62							1.0830462-3.2619149	-.1929779						
	70.000														
710	63							1.0997358-3.2618091	-.0256761						
	70.000														
720	64							1.1142966-3.2402622	-.3357601						
	70.000														
730	65							1.1452837-3.2401834	-.2063931						
	70.000														
740	66							1.1613041-3.2401047	-.0743408						
	70.000														
(S,C OR RETURN)>															
	1234	56789	1234	56789	1234	56789	1234	56789	1234	56789	1234	56789	1234	56789	1234
750	67							1.1888861-3.2186494	-.3055537						
	70.000														
760	68							1.2075308-3.2185239	-.2200953						
	70.000														
770	69							1.2200413-3.2183983	-.1335330						
	70.000														
780	70							1.2634673-3.1968262	-.2654222						
	70.000														
790	71							1.2695847-3.1967588	-.2342216						
	70.000														
800	72							1.2749318-3.1966915	-.2028807						
	70.000														
810	73	1	1	1	1	1	1	.8787037-3.5446358	-.5682845						
	70.000														
820	74	1	1	1	1	1	1	.9813550-3.5448013	-.3600641						
	70.000														
830	75	1	1	1	1	1	1	1.0383987-3.5449667	-.1342854						
	70.000														
840	76							.9556396-3.5215521	-.5715815						
	70.000														
(S,C OR RETURN)>															

	123456789	123456789	123456789	123456789	123456789	123456789	123456789	1234
56789								
850	77						1.0444118-3.5215666	-.3862172
	70.000							
860	78						1.0976054-3.5215812	-.1876949
	70.000							
870	79						1.0325396-3.4984790	-.5748770
	70.000							
880	80						1.1073122-3.4983428	-.4126808
	70.000							
890	81						1.1567846-3.4982065	-.2410796
	70.000							
900	82						1.1142402-3.4751546	-.5663933
	70.000							
910	83						1.1703313-3.4750532	-.4387410
	70.000							
920	84						1.2118531-3.4749518	-.3056425
	70.000							
930	85						1.1990483-3.4518771	-.5473019
	70.000							
940	86						1.2332332-3.4517915	-.4650465
	70.000							
(S,C OR RETURN)>								
	123456789	123456789	123456789	123456789	123456789	123456789	123456789	1234
56789								
950	87						1.2617830-3.4517060	-.3806732
	70.000							
960	88						1.2857970-3.4286330	-.5179480
	70.000							
970	89						1.2959437-3.4285464	-.4918856
	70.000							
980	90						1.3055622-3.4284599	-.4656248
	70.000							
990	5	40	1					
1000	1	30000000.		.3	.283	.0000073		
1010		386.						
1020								
1030								
1040								
1050								
1060								
1070	1	1	2	20	19	4	5	23
	70.							22
1080	5	13	14	32	31	16	17	35
	70.							34
(S,C OR RETURN)>								

123456789 123456789 123456789 123456789 123456789 123456789 123456789 1234
56789

1090	6	19	20	38	37	22	23	41	40	2	1	3
	70.											
1100	10	31	32	50	49	34	35	53	52	2	1	
	70.											
1110	11	37	38	56	55	40	41	59	58	2	1	3
	70.											
1120	15	49	50	68	67	52	53	71	70	2	1	
	70.											
1130	16	55	56	74	73	58	59	77	76	2	1	3
	70.											
1140	20	67	68	86	85	70	71	89	88	2	1	
	70.											
1150	21	2	3	21	20	5	6	24	23	2	1	3
	70.											
1160	25	14	15	33	32	17	18	36	35	2	1	
	70.											
1170	26	20	21	39	38	23	24	42	41	2	1	3
	70.											
1180	30	32	33	51	50	35	36	54	53	2	1	
	70.											

(S,C OR RETURN)>

123456789 123456789 123456789 123456789 123456789 123456789 123456789 1234
56789

1190	31	38	39	57	56	41	42	60	59	2	1	3
	70.											
1200	35	50	51	69	68	53	54	72	71	2	1	
	70.											
1210	36	56	57	75	74	59	60	78	77	2	1	3
	70.											
1220	40	68	69	87	86	71	72	90	89	2	1	
	70.											
1230	4	1		.2459		.5216		-.8170				
1240	6	2		-.6033		-.7862		.1338				
1250	7	3		.3740		.5638		-.7364				
1260	9	4		-.5703		-.8077		.1497				
1270	10	5		.4556		.5940		-.6631				
1280	12	6		-.2475		.2416		-.9383				
1290	13	7		.5149		.6190		-.5930				
1300	15	8		-.3479		.2139		-.9128				
1310	16	9		.5594		.6410		-.5256				
1320	18	10		-.4396		.1876		-.3784				
1330	22	11		.1002		.5567		-.8246				
1340	24	12		-.6334		-.7652		.1154				

(S,C OR RETURN)>

123456789 123456789 123456789 123456789 123456789 123456789 123456789 1234
56789

1350	25	13	.2328	.5959	-.7686
1360	27	14	-.6025	-.7875	.1297
1370	28	15	.3222	.6243	-.7117
1380	30	16	-.4116	.2801	-.8672
1390	31	17	.3899	.6477	-.6546
1400	33	18	-.5045	.2536	-.8253
1410	34	19	.4433	.6682	-.5975
1420	36	20	-.5874	.2286	-.7763
1430	40	21	-.0425	.5924	-.8045
1440	42	22	-.3572	.3740	-.8559
1450	43	23	.0905	.6285	-.7725
1460	45	24	-.4680	.3453	-.8134
1470	46	25	.1845	.6548	-.7329
1480	48	26	-.5621	.3190	-.7630
1490	49	27	.2580	.6767	-.6896
1500	51	28	-.6436	.2943	-.7065
1510	52	29	.3183	.6958	-.6439
1520	54	30	-.7150	.2708	-.6446
1530	58	31	-.1771	.6284	-.7574
1540	60	32	-.5153	.4086	-.7533

(S,C OR RETURN)>

123456789 123456789 123456789 123456789 123456789 123456789 123456789 1234
56789

1550	61	33	-.0481	.6613	-.7486
1560	63	34	-.6112	.3828	-.6927
1570	64	35	.0468	.6855	-.7265
1580	66	36	-.6909	.3588	-.6276
1590	67	37	.1239	.7057	-.6976
1600	69	38	-.7585	.3360	-.5584
1610	70	39	.1887	.7233	-.6643
1620	72	40	-.8157	.3141	-.4859
1630	76	41	-.2984	.6649	-.6848
1640	78	42	-.6517	.4435	-.6153
1650	79	43	-.1779	.6943	-.6974
1660	81	44	-.7286	.4209	-.5404
1670	82	45	-.0850	.7163	-.6926
1680	84	46	-.7911	.3994	-.4633
1690	85	47	-.0073	.7347	-.6784
1700	87	48	-.8419	.3787	-.3844
1710	88	49	.0598	.7506	-.6580
1720	90	50	-.8826	.3587	-.3040

1730
1740

(S,C OR RETURN)>

123456789 123456789 123456789 123456789 123456789 123456789 1234
56789

1750
1760
1770
1780
1790
1800
1810
1820
1830
1840
1850
1860
1870
1880
1890
1900
1910
1920
1930
1940

(S,C OR RETURN)>

123456789 123456789 123456789 123456789 123456789 123456789 1234
56789

1950
1960
1970
1980
1990
2000
2010
2020
2030
2040
2050
2060
2070
2080
2090
2100
2110
2120
2130
2140

(S,C OR RETURN)>

123456789 123456789 123456789 123456789 123456789 123456789 123456789 1234
56789

2150

2160

2170

2180

2190

2200

2210

2220

2230

2240

2250 0

2260 EOI

>

APPENDIX B

DEFLECTION AND SLOPE AT POINT B

Referring to Fig. 2-7, one obtains the reaction force at c from $\Sigma (M_z)_C = 0$:

$$R_C = \frac{M_0 - P(d - L)}{d - c} \quad (B.1)$$

where $(M_z)_C$ is the moment about z axis through point C.

To obtain the deflection and slope at B, the beam is divide into 2 portions.

$$(1) \quad c < x < d$$

Considering the equilibrium of the portion of the beam to the right of point C (Fig. B-1), one can obtain

$$M_1 = (P + R_C)x - PL - R_Cc - M_0 \quad (B.2)$$

The moment of inertia of the cross sectional area with respect to the neutral axis is

$$I_1 = \frac{\pi(r_s^4 - r_i^4)}{4} \quad (B.3)$$

Let E be the modulus of elasticity, the differential equation of the elastic line for the beam is

$$\begin{aligned}
 y'' &= - \frac{M_1}{EI_1} \\
 &= - \frac{[(P + R_C)x - (PL + R_Cc + M_0)]}{EI_1}
 \end{aligned}
 \tag{B.4}$$

Let

$$A_1 = - \frac{(P + R_C)}{EI_1} \tag{B.5}$$

$$A_2 = \frac{(PL + R_Cc + M_0)}{EI_1} \tag{B.6}$$

Then

$$y'' = A_1x + A_2 \tag{B.7}$$

Separating variables and integrating twice one obtains

$$y = \frac{A_1}{6}x^3 + \frac{A_2}{2}x^2 + C_1x + C_2 \tag{B.8}$$

where C_1 and C_2 are constants of integration.

The integration constants are determined from the conditions:

$$y = 0 \text{ at } x = c \text{ and } x = d$$

Substituting these conditions into the equation (B.8), one obtains

$$C_1 = -\frac{1}{6}[A_1(c^2 + cd + d^2) + 3A_2(c + d)] \quad (B.9)$$

$$C_2 = \frac{cd}{6}[A_1(c + d) + 3A_2] \quad (B.10)$$

With these values, the slope at $x = c$ can be obtained

$$y'_c = \frac{c}{2}(A_1c + 2A_2) + C_1 \quad (B.11)$$

$$(2) \quad b < x < c$$

Fig. B-2 is a free body diagram of the portion of the beam to the right of point B. One obtains

$$M_2 = P(x - L) - M_0 \quad (B.12)$$

$$I_2 = I_1 = \frac{\pi(r_s^4 - r_i^4)}{4}$$

The differential equation is

$$\begin{aligned} y'' &= -\frac{M_2}{EI_1} \\ &= \frac{-Px + (PL + M_0)}{EI_1} \end{aligned} \quad (B.13)$$

Let

$$A_3 = -\frac{P}{EI_1} \quad (B.14)$$

$$A_4 = \frac{PL + M_0}{EI_1} \quad (B.15)$$

Then

$$y'' = A_3x + A_4 \quad (B.16)$$

$$y' = \frac{A_3}{2}x^2 + A_4x + C_3 \quad (B.17)$$

$$y = \frac{A_3}{6}x^3 + \frac{A_4}{2}x^2 + C_3x + C_4 \quad (B.18)$$

At $x = c$, $y = 0$ and $y' = y'_C = \frac{c}{2}(A_3c + 2A_4) + C_3$,
one obtains

$$C_3 = y'_C - \frac{c}{2}(A_3c + 2A_4) \quad (B.19)$$

$$C_4 = -\frac{c}{6}(A_3c^2 + 3A_4c + 6C_3) \quad (B.20)$$

Then the deflection and slope of point B can be
obtained

$$y_B = \frac{b}{6}(A_3b^2 + 3A_4b + 6C_3) + C_4 \quad (B.21)$$

$$y'_B = \frac{b}{2}(A_3b + 2A_4) + C_3 \quad (B.22)$$

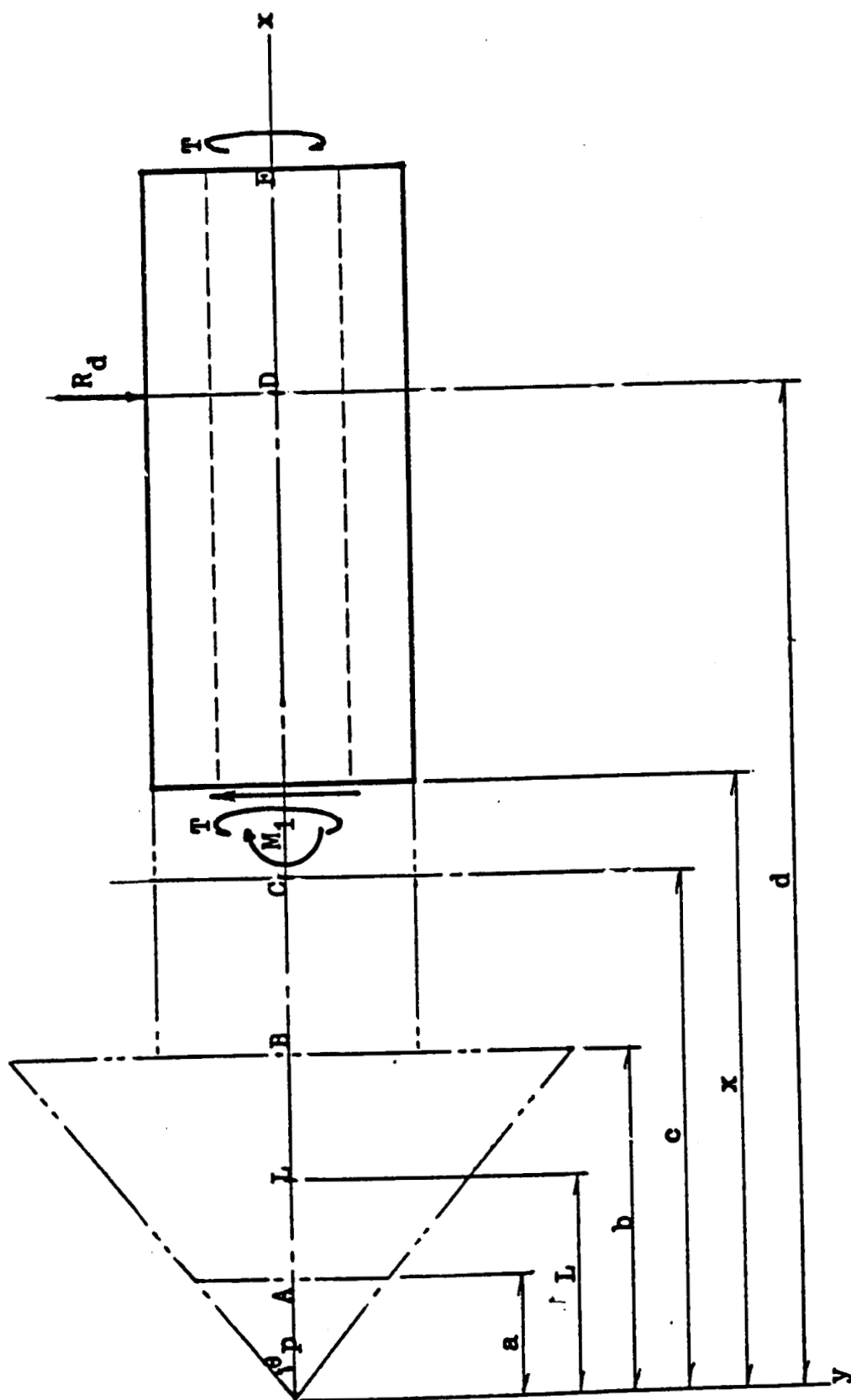


Fig. B-1 Free body diagram of the beam to the right of point C

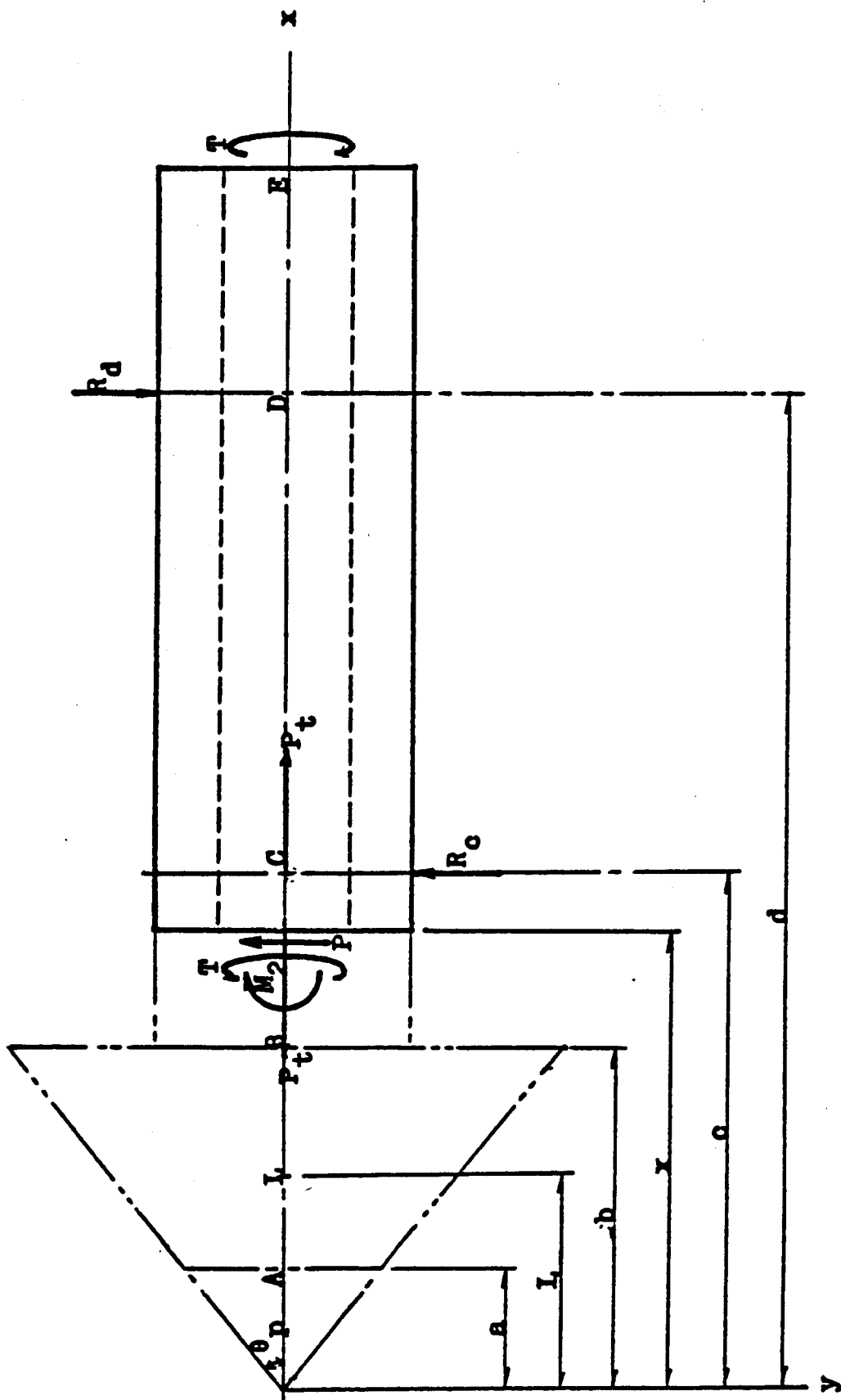


Fig. B-2 Free body diagram of the beam to the right of point B

1. Report No. NASA CR-179620 AVSCOM TR-87-C-16		2. Government Accession No.		3. Recipient's Catalog No.	
4. Title and Subtitle A Simplified Computer Solution for the Flexibility Matrix of Contacting Teeth for Spiral Bevel Gears				5. Report Date June 1987	
				6. Performing Organization Code	
7. Author(s) C.Y. Hsu and H.S. Cheng				8. Performing Organization Report No. None	
				10. Work Unit No. 1L161102AH45 505-63-51	
9. Performing Organization Name and Address Northwestern University Evanston, Illinois 60201				11. Contract or Grant No. NSG-3143	
				13. Type of Report and Period Covered Contractor Report Final	
12. Sponsoring Agency Name and Address U.S. Army Aviation Research and Technology Activity - AVSCOM, Propulsion Directorate, Lewis Research Center, Cleveland, Ohio 44135 and NASA Lewis Research Center, Cleveland, Ohio 44135.				14. Sponsoring Agency Code	
15. Supplementary Notes Project Manager, John J. Coy, Propulsion Directorate, U.S. Army Aviation Research and Technology Activity - AVSCOM, Lewis Research Center.					
16. Abstract A simplified analysis for obtaining the flexibility matrix of the contacting teeth of a pair of spiral bevel gears is presented. An existing finite element code SAP IV was used for computing the tooth deformation. The total deformation is obtained by superimposing the tooth deformation on the shaft deformation which was obtained from conventional beam theory. This simplified analysis was incorporated in the main computer code developed earlier by Chao (NASA CR-4077) for computing dynamic loads in spiral bevel gears.					
17. Key Words (Suggested by Author(s)) Gears; Transmissions; Machine design; Vibration			18. Distribution Statement Unclassified - unlimited STAR Category 37		
19. Security Classif. (of this report) Unclassified		20. Security Classif. (of this page) Unclassified		21. No. of pages 72	
				22. Price* A04	